DEVELOPMENT AND EVALUATION OF A METHOD TO CHARACTERIZE THE SOLUBILITY OF HIGH-PROTEIN DAIRY POWDERS USING AN ULTRASONIC FLAW DETECTOR

by

MARY HAUSER

B.S., Kansas State University, 2013

A THESIS

submitted in partial fulfillment of the requirements for the degree

MASTER OF SCIENCE

Food Science

KANSAS STATE UNIVERSITY
Manhattan, Kansas

2015

Approved by:

Major Professor
Jayendra Amamcharla

Copyright

Abstract

High-protein dairy powders are added to a variety of products to improve nutritional, functional, and sensory properties. To have the intended properties, the powder must be soluble. The solubility is effected by processing storage, and dissolution conditions, as well as the type of powder. Various tests are used to determine solubility, but they are time-consuming and subjective. Literature has shown that ultrasound spectroscopy can characterize the solubility of high-protein dairy powders, but it requires expensive equipment and skilled technicians. An economical alternative is to use an ultrasonic flaw detector, which is commonly used in the construction industry. For this study, an ultrasonic flaw detector based method was developed to characterize the solubility of high protein dairy powders. To evaluate the method, commercially available milk protein concentrate (MPC) was obtained and stored at 25°C and 40°C and stored for four weeks to produce powders with different dissolution properties. To test the powders, a 5% (w/w) concentration of powder was added to water. A focused beam reflectance measurement (FBRM) and solubility index were used as a reference method. After powder addition, data was collected at regular intervals for 1800s. The FBRM and solubility index showed that the powders lost solubility as the storage time and temperature increased. From the ultrasound data, one parameter was extracted from the relative velocity and three parameters were extracted from the attenuation data. A soluble powder had a low relative velocity standard deviation from 900-1800s, high area under the attenuation curve, low peak time, and high peak height. The ultrasonic flaw detector detected differences in solubility before the solubility index. When testing MPC with protein contents ranging from 85% to 90% and at a dissolution temperature of 40°C and 48°C, data from the ultrasonic flaw detector and FBRM showed that the solubility decreased as the protein content increased and increasing the dissolution temperature

improved the solubility of the powder. Overall, the ultrasonic flaw detector can characterize the solubility of high-protein dairy powders.

Table of Contents

List of Figures

List of Tables

Acknowledgements

I would like to thank Dr. Jay, Dr. Schmidt, and Dr. Smith for serving on my committee. I Thank you to family, friends, Food Science Institute faculty and staff, and the other graduate students here at K-State for your support. Finally, I would like to thank the Midwest Dairy Foods Research Center (St. Paul, MN), R.E. French Scholarship, and Winslow scholarship for their financial support.

Dedication

I would like to dedicate my work to family, friends, and lab/office mates for their support. I would also like to dedicate my work to God for all that He has done for me.

Chapter 1 - Introduction

High-protein dairy powders have a higher protein content and lower lactose content than skim milk powder. Milk protein concentrate (MPC), milk protein isolate (MPI), whey protein concentrate (WPC), and whey protein isolate (WPI) are the commonly used high-protein dairy powders. MPC does not have a standard of identity, but does have GRAS notification (GRAS Notice No. GRN 000504). With MPC, MPI, WPC, and WPI, a concentrate has up to 85% protein content and an isolate has a protein content of 90%. The name of the powder indicates the protein content of the powder. For example MPC80 and WPI90 have a protein content of 80% and 90%, respectively. These powders are typically added to protein bars and beverages, processed cheese, and a variety of dairy and foods products to improve the nutrition, sensory, and functional properties of the finished product. The United States has the world's largest market for MPC. In the United States, the production of MPC has doubled over the past eight years. New Zealand, Australia, and European Union are the leading exporters of MPC.

In choosing a high-protein dairy powder, beverage processors consider the solubility of the powder as one of the criteria. A low soluble powder is prone to clog pipes and filters, form sediment, and does not provide the intended functional and nutritional characteristics for the finished product. The solubility of high-protein dairy powders is affected by the processing, storage, and dissolution conditions, as well as the composition of the powder. Studies have shown that increasing the inlet and outlet drying temperature decreases the solubility of high-protein dairy powder. During storage, an increase in storage temperature and an extended storage period leads to a reduction in solubility. An increase in dissolution temperature and stirring speed has been shown to improve the solubility of high-protein dairy powders. However, limited

research has been conducted to determine how the protein and lactose content affect the solubility of high-protein dairy powders.

With so many factors affecting solubility, a variety of methods are used to characterize the solubility of high-protein dairy powders. However, these methods are time-consuming, difficult to reproduce, and require expensive equipment and skilled technicians. Low-intensity ultrasound has the advantage of being rapid, precise, and non-destructive. Literature has shown that ultrasound spectroscopy has the ability to detect differences between various dairy products and dairy based powders. However, ultrasound spectroscopy requires expensive equipment and skilled technicians. An economical alternative is to use an ultrasonic flaw detector (UFD). The UFD is widely used in the construction industry to detect flaws and defects in metal and structures. The following chapters focus on developing and evaluating an UFD based method to characterize the solubility of high-protein dairy powders.

Chapter 2 - Literature Review

High-protein dairy powders improve the nutritional, sensory, and functional properties of various food products. These powders can have a protein content as low as 25% and as high as 90%. One important property of high-protein dairy powders is the solubility. Solubility is affected by processing, storage, and dissolution conditions, as well as the composition of the powder. Various methods are used to determine the solubility of a powder and low-intensity ultrasound has the potential to be a routine method. Low-intensity ultrasound is sensitive to the composition and structure of a food product. In the dairy foods industry, low-intensity ultrasound has characterized dairy based powders, milk, and cheese. This literature review focuses on the solubility of high-protein dairy powders and how low-intensity ultrasound has been used in the dairy foods industry.

Overview of high-protein dairy powders

High-protein dairy powders provide more dairy flavor and protein with less lactose. Commonly used types of powder include milk protein concentrate (MPC), milk protein isolate (MPI), whey protein concentrate (WPC), and whey protein isolate (WPI). Table 2-1 compares the composition of skim milk powder, MPC, and WPC.

Table 2-1 Composition for skim milk powder, MPC, and WPC

	Powder					
Component	Skim milk	MPC70	MPC80	MPI90	WPC80	WPC90
Protein	36	70	80	90	80	90
Ash	7.7	7	7	6	3	1
Fat	1	1.5	1.5	1.5	4	3
Lactose	51.3	16	7	1	4	1

Composition obtained from Abd et al. (2009);Agarwal et al. (2015)

As can be observed, the increase in protein content typically leads to a reduction in lactose. The ash and fat content experience little change. The WPC has reduction in ash as the protein content increases.

MPC does not have a standard of identity, but it does have GRAS notification (Agarwal et al., 2015). MPC is typically described as a concentrated source of casein and whey proteins in the same ratio as they are found in milk (Chandan and Kilara, 2011; Agarwal et al., 2015). The American Dairy Products Institute and U.S. Dairy Export Council describe MPC as having a minimum crude protein content of 40% and MPI as having a minimum crude protein content of 90% (FDA, 2014). WPC has a minimum protein content of 25% and WPI has a minimum protein content of 90% (Chandan and Kilara, 2011).

Nutritional drinks and bars, protein fortified foods and beverages, and infant formula contain MPC and WPC (Chandan and Kilara, 2011; Agarwal et al., 2015). Manufacturers use 1% to 10% MPC or MPI in products and high-protein products contain up to 15% MPC or MPI. Powdered beverage mixes can contain 80% to 90% MPC or MPI (FDA, 2014). Nutritional bars containing high-protein dairy powders increase in hardness during storage (Agarwal et al., 2015). In some countries, MPC and WPC are added to yogurt and cheese. During the production of cheese that do not have a standard of identity, manufacturers add MPC to standardize the milk. One study found that the addition of MPC to cheese increased the yield from 13.8% to 16.7%. MPC has also been added to ice cream to reduce the lactose (Agarwal et al., 2015). MPC and WPC provide an increase in water binding, viscosity, gelling, foaming/whipping, and emulsification. To be able to achieve these functional properties, the powder must be soluble (Chandan and Kilara, 2011). The following section focuses on the solubility of MPC and WPC.

Solubility of high-protein dairy powders

Manufacturers consider the solubility of a powder when selecting a high-protein dairy powder. If a powder is insoluble, filters and pipes can become clogged, a sedimentation layer can form, and the product will not have the desired functional and nutritional properties (Chandan and Kilara, 2011). A poor soluble powder can increase operating costs, too. To decrease operating costs, manufacturers want to dissolve powders as fast as possible at a low temperature and with as little stirring as possible (Mimouni et al., 2010a). The solubility of a powder depends on factors such as processing, storage, and dissolution conditions, as well as the composition of powder.

Effects of processing conditions on solubility

MPC and WPC are produced in similar ways. MPC starts as skim milk and WPC is produced from the whey formed during cheese production or acidification of milk to form casein. The type of whey used can influence the properties of the final product. The skim milk or whey goes through ultrafiltration and diafiltration to remove water, lactose, and salt without denaturing the protein. Ion exchange chromatography is used to produce a high-purity whey protein. After the filtration process, the retentate is vacuum evaporated and spray dried (Chandan and Kilara, 2011).

Fang et al. (2012) found that increasing the inlet air temperature led to a decrease in solubility. During processing, the high temperature denatures the protein, leading to aggregation and bonds forming between whey and casein. When the proteins denature, they begin to unfold and expose the hydrophobic bonds, which prevent the powder from rehydrating properly. Some processing steps can be added to improve the solubility of MPC. These steps include ion exchange to remove calcium, adding salt during diafiltration, or high-pressure processing (Gazi

and Huppertz, 2015). Adding a lactose or sodium solution during processing also improves the solubility of the final powder (Schuck et al., 2007).

Effects of storage conditions on solubility

Fresh powders have the best solubility (Fang et al., 2011; Gazi and Huppertz, 2015). The solubility of a powder changes over the storage period. Time, temperature, and relative humidity affect the solubility of high-protein dairy powders, and these storage conditions affect MPC more than WPC. Increasing the storage temperature decreases the solubility of MPC (Anema et al., 2006; Fang et al., 2011, Fyfe et al., 2011; Gazzi and Huppetz, 2015) When studying the solubility of MPC with a focused beam reflectance measurement (FBRM), the dissolution rate decreased and the final particle size increased as the solubility decreased for MPC stored at higher storage temperatures (Fang et al., 2011). Anema et al. (2006) provided a detailed description of how a storage temperature of 20 °C, 30 °C, 35 °C, 40 °C, and 50 °C affected the solubility of MPC. A storage temperature of 20 °C did not result in a change in solubility After 10 days of storage at 30°C, a gradual reduction in solubility was noticed. Powders stored at 35 °C, 40 °C, and 50 °C reached a minimum solubility of 20%. The amount of whey in the powder was equal to the minimum solubility. However, the time to reach the minimum solubility decreased with an increase in storage temperature. Powders stored at 35 °C took about 38 days to reach the minimum value and powders stored at 50 °C took approximately 13 days.

Besides temperature, storage time affects the solubility of a powder. Anema et al. (2006) noticed that the solubility decreased as the storage time increased at all storage temperatures. Fang et al. (2011) stated that the storage time magnifies the changes that occur due to an increased storage temperature. Relative humidity is one more storage condition to monitor. Fyfe

et al. (2011) mentioned that increasing the relative humidity reduced the solubility of MPC. Storage induced changes in solubility are commonly attributed to the casein.

Lactose and whey do not experience significant changes in solubility during storage (Mimouni et al., 2010b; Gazi and Huppertz, 2015). Hsu and Fennema (1988) found that storing WPC at or below 20 °C led to no or a slight increase of solubility for 6 months of storage. When storing the powder at 40 °C, a 7% reduction in solubility was noticed after 3 months. Gazi and Huppertz (2015) found that whey only affected the solubility of high-protein MPC powder that has been stored at 50 °C for 3 or 4 weeks. A more detailed description of how casein and other components of a high-protein dairy powder affect the solubility will be provided in a later section.

Effects of dissolution condition on solubility

Even if changes occur during storage, dissolution conditions such as stirring speed and dissolution temperature can improve the solubility of the powder. Studies that observed the effects of dissolution conditions on solubility focused on the dissolution of native phosphocaseinate or MPC because they have slower dissolution rates. Jeantet et al. (2010) and Richard et al. (2013) determined that increasing the stirring speed shortened the rehydration time. When the speed increased from 700 rpm to 900 rpm, a 25% reduction in rehydration time was noticed (Riachrd et al., 2013). A higher stirring speed was needed when the solids concentration increased (Jeantet et al., 2010).

Besides stirring speed, the dissolution temperature influenced the dissolution of high-protein dairy powders. In general, increasing the dissolution temperature shortened the rehydration time. An increase in dissolution temperature led to the ability to better distinguish between fresh and aged powders, which would have different dissolution properties (Fang et al.,

2011) However, the dissolution temperature could only be raised so far. With native phosphocaseinate, the solubility decreased at 37 °C. (Richard et al., 2013). At 60 °C, the dissolution time increased for MPC and the best dissolution temperature for MPC was determined to be 50 °C (Fang et al., 2010; Fang et al., 2011). Pelegrin and Gomes (2012) tested the solubility of WPC at temperatures from 40 °C and 90 °C and found that the solubility decreased as the temperature increased. Fang et al. (2010) and Richard et al. (2013) attributed the reduction in solubility at a particular temperature to the denaturation and aggregation of proteins.

Jeantet et al. (2010) and Richard et al. (2013) noticed that raising the dissolution temperature was more effective at reducing the reconstitution time than increasing the stirring speed. The dissolution medium has been shown to affect the solubility of MPC and MPI, too. Crowley et al. (2015) noticed that the solubility improved when MPC or MPI was dissolved in milk or a sodium solution. Increasing the reconstitution time increases the soluble material for powders with a slower dissolution rate (Gazi and Huppertz, 2015).

Effects of powder composition on solubility

The composition of the powder is the last factor that determines how soluble a powder is. MPC has a short wetting and long dispersion time, whereas WPC has a long wetting time and short dispersion time (Schuck et al, 2007). Casein, calcium, magnesium, and phosphorus are the slowest-dissolving portions of MPC. Increasing any of these components will decrease the solubility of a powder (Mimouni et al., 2010b; Sikand et al., 2011). Colloidal calcium prevents the micelle from breaking apart (Mimouni et al., 2010a).To improve the solubility of MPC, sodium, sodium citrate, or sodium phosphate can be added before spray drying (Schuck et al., 2007). Sodium has the ability to solubilize κ-casein (Sikand et al., 2011).

The addition of whey during the drying process also improves the solubility of casein. Gaini et al. (2007) found that codrying casein with 12% whey improved the solubility. Whey protein prevented the casein micelles from interacting with each other. If the whey denatured during the drying process, then the β-lactoglobulin unfolded and bonded to the casein (Sharma et al., 2012). Sikand et al. (2011) focused on what proteins caused the insolubility of MPI, and whey did not affect the solubility. They found a more soluble powder contained less α_{s1} and κ-casein.

As mentioned in a previous section, casein typically decreased the solubility of a powder, and storage conditions affected the casein. Therefore, many studies have worked with MPC or casein powders to determine what changes in casein cause a reduction in solubility. Studies typically focused in the surface of the powder particles and the interactions between the proteins. Fyfe et al. (2011), Crowley et al., (2015), and Gazi and Huppertz (2015) mentioned that a crust or skin formed during storage that further reduced the water transfer rate for casein. Increasing the agitation or rehydration time has been shown to completely or partially remove the skin (Mimouni et al., 2010a).

With or without a crust, the water transfer rate decreased the solubility of a powder and not the formation of insoluble material (Mimouni et al., 2009). The loss of solubility was attributed to an increase in hydrophobicity (Mimouni et al., 2009; Fyfe et al., 2011; Crowley et al., 2015). Intermicellar bonds, which are non-polar, caused the hydrophobicity (Mimouni et al., 2010a; Fyfe et al., 2011). Increasing the storage time and temperatures leads to an increase of crosslinking between casein and a reduction in solubility (Anema et al., 2006; Fang et al., 2011).

The interactions between the caseins changed with the composition of the powder (Mimouni et al., 2010a; Gazi and Huppertz, 2015). Studies have shown that increasing the

amount of lactose or adding ultrafiltrate during production led to an increase in solubility (Gaiani et al., 2005; Gaini et al., 2006; Schuck et al., 2007; Richard et al., 2013). Richard et al. (2013) mentioned that lactose is fast dissolving and helped water enter the core of the powder particle. During storage, the casein becomes lactosylated and the solubility decreased (Anema et al., 2006).

WPC has been shown to be a more soluble powder. However, WPC becomes insoluble when the protein is denatured during drying (Fang et al., 2010; Gazi and Huppertz, 2015). With WPC, the solubility of powder is affected by the pH of the product. WPC is least soluble at a pH of 5.2, which is the isoelectric point of whey. The whey has no charge and they are attracted to each other. When the pH is above or below the isoelectric point, the whey has either a positive or negative charge. The whey proteins repel each other and they interact with the water (Pelegrine and Gasparetto, 2005; Pelegrine and Gomes, 2012).

WPC is commonly used in high-protein beverages. Unfortunately, the high-processing temperatures leads to aggregation of the whey and the protein sediments outs. Whey begins to denature at a temperature around 70 °C (Ashokkumar et al., 2009). Therefore, manufacturers are conducting research to produce heat stable WPC. Reducing the size of the whey proteins and adding sugar have been shown to increase the heat stability of WPC.

Microparticulated WPC are aggregates of native protein with soluble and insoluble proteins that have a controlled size. They are produced by aggregating the protein and then high-shear and high-pressure conditions are used. These microparticulated WPC powders enhance the heat stability since the protein have a fewer active sites for aggregation and they have a lower proportion of undenatured proteins (Fuller, 2015). Koh et al. (2014) noticed that high-shear mixing and homogenization increased the heat stability of whey proteins. Ultrasound can also

improve the heat stability of whey (Ashokkumar et al., 2009; Koh et al., 2014). The ultrasound reduces the size of the particle to approximately 1μm in a solution (Koh et al., 2014). The ultrasound has the ability to break apart the hydrophobic bonds and intermolecular disulfide bonds by an implosion caused by the change in pressure from the ultrasound wave (Ashokkumar et al., 2009).

One popular way to increase the heat stability of whey is to add various types of sugar. Glycation is one way to improve heat stability (Liu and Zhong, 2015). Liu and Zhong (2015) found that a temperature of 130 °C for 30 minutes and relative humidity of 79% shorten the glycation process for WPI. They found that lactose reacted better than maltodextrin and that both types of sugar improved the heat stability. In general, lactose (Rich and Foegeding, 2000; Liu and Zhong, 2015) and sucrose (Kulmyrzaz et al., 2000) improves the heat stability and ribose does not improve the heat stability (Rich and Foegeding, 2000)

Testing the solubility of high-protein dairy powders

A variety of tests exist to measure the solubility of powders. Table 2.2 provides a summary of some of the tests that were found in literature. One of the promising methods for determining solubility is ultrasound spectroscopy. The following section describes the history of ultrasound, types of ultrasound tests, and how ultrasound has been used in the food industry, with focus given to the dairy foods industry.

Overview of ultrasound

History of low-intensity ultrasound

Ultrasound equipment was first developed during World War I to detect submarines. The equipment was further developed during World War II and served as the basis for current ultrasound equipment for non-destructive testing in the construction and medical industry. In the

1960s, the Surface Acoustic Wave system was developed and now is typically used in the electronics and bioelectronics industry. Over time, the cost of ultrasound equipment has decreased, which led to research on how the food industry can use ultrasound in factory and laboratory settings (Povey and McClements, 1988).

In 1948, Winder first mentioned ultrasound being used for food analysis by using a "sing-around" technique to use velocity to determine the fat content in milk and alcohol content in wine samples. Other low-intensity ultrasound research focused on characterizing gels and glucose solutions, and the first complex food thoroughly examined was eggs. With the eggs, ultrasound determined the shell thickness and the quality of the egg's yolk and white. Eventually, researchers started to apply ultrasound for monitoring flow rates, inspecting meats, and determining the solids content of a sample (Povey, 1989). Overall, the use of ultrasound in the food industry is a relatively young science (Pico, 2012).

Ultrasound background

Ultrasound is sound waves that have a frequency above the human hearing of 20 kHz. Literature classifies ultrasound as high-intensity and low-intensity ultrasound. High-intensity ultrasound operates at a power above $1 W/cm^2$ and a frequency between 20 and 100 kHz. Manufacturers use high-intensity ultrasound for cleaning, dehydrating, freezing, and other processes because the ultrasound wave has the ability to alter the physical and chemical properties of a product. New and novel products can be developed with high-intensity ultrasound. When the power is below $1 W/cm^2$ and the frequency is above 100 kHz, ultrasound is classified as low-intensity. Low-intensity ultrasound is used for quality testing because the wave does not alter the physical or chemical properties of the sample (Pico, 2012). To determine the

quality of the product, a researcher collects and examines ultrasound data such as velocity and attenuation. The remainder of the literature review focuses on low-intensity ultrasound.

Advantages and disadvantages of ultrasound testing

Current analytical testing methods are subjective, difficult to reproduce, time-consuming, and destructive. Studies have focused on replacing current analytical tests, such as the visual reconstitution test for dissolution and the Irish Dairy Board method for heat stability testing. Alternative methods that have been tested include nuclear magnetic resonance (NMR) for dissolution and nitrogen content for heat stability testing. These methods help quantify the results, but the methods still require expensive equipment, skilled technicians, sample preparation and destruction, and cannot test optically opaque samples (Lehmann and Buckin, 2005; Fang, Selomulya and Chen, 2008). Low-intensity ultrasound can replace current analytical methods because ultrasound does not have these disadvantages. Low-intensity ultrasound tests have the advantage of being rapid, precise, automated, and sensitive to small changes in a sample. Samples for low-intensity ultrasound testing rarely need any preparation and are not destroyed (Chandrapala et al., 2012).

However, low-intensity ultrasound tests have some limitations. Plant tissues, aerated foods, foods with semi-crystalline fat, and naturally complex food are highly attenuating and cannot be tested with low-intensity ultrasound. The amount of air or air bubbles in a sample must be monitored because air reduces the ultrasound signal. Changes in temperature, ingredient concentration, and the environment limits the use of low-intensity ultrasound in a plant setting. A laboratory setting can assist with controlling the temperature, ingredient concentration, and environment. Whether the ultrasound is being used in a plant or laboratory setting, the testing temperature must remain low so as not to ruin the equipment (Coupland, 2004). Overall, the

natural complexity of food limits the use of ultrasound, but new equipment and technology can improve the ultrasound's ability to characterize food (Awad et al., 2012).

Velocity

Velocity is the speed of the wave as it travels through the sample. Tests commonly use the distance the wave travels (*d*) and the time-of-flight (*t*) to calculate the velocity with the following equation:

$$V=d/t$$

Povey and McClements (1988) stated that velocity is accurate and can be easily reproduced. For food products, the velocity ranges from 1000 m/s to 2000 m/s and properties of the sample such as concentration of a substance, density, changes in composition, and elastic properties of a sample influence the velocity (Pico, 2012). Sensitivity to changes in composition makes velocity an important measurement for changes that may occur in a sample.

For example, Benedito et al. (2001) mentioned that various physical, microbial, and chemical processes occur while the cheese matures, and these changes increase the difficulty for determining the maturity of the cheese. Benedito et al. (2000) and Benedito et al. (2001) characterized the maturity of Mahon cheese with velocity. They noticed that the velocity increased as the cheese aged. The increasing velocity is attributed to an increase in the bulk modulus of the cheese. Benedito et al. (2000) said fresh cheese should be around 1630m/s and Benedito et al. (2001) reported a velocity of 1670 m/s. With mature cheese, Benedito et al. (2000) measured the velocity at 1740 m/s and Benedito et al. (2001) noted that the velocity was greater than 1680 m/s. The differences in the velocity for fresh cheese and mature cheese can be attributed to the variation between the batches, composition of the milk, and small variation in storage conditions.

The testing temperature influences the velocity reading, too. A 1 °C increase in water temperature increased the velocity by 2.4 m/s. With milk, the velocity decreases as the temperature increases. (Dukhin et al., 2005).Therefore, the testing temperature should remain constant to obtain accurate readings. The temperature has the ability to help determine the composition of a product by using the relationship of the velocity for the component and the temperature of the product.

For example, Mulet et al. (1999) proposed that to determine the fat content of cheese, the sample temperature must be between 0 °C and 17 °C. Temperatures above 18.5 °C were not suitable for compositional analysis because the fat did not affect the velocity. In the temperature range of 3 °C to 9 °C the velocity was affected by the amount of fat in the sample, with the velocity increasing as the amount of fat in a sample increased. At this temperature range, the fat had a higher velocity than water (Tellis-Romero et al., 2011). When the temperature was between 17 °C and 25 °C, the velocity rapidly changed and the fat began to "oil out" (Benedito et al., 1999; Mulet et al., 1999). When the temperature was between 24 °C and 29 °C, samples containing more fat had a lower velocity. At this temperature range, the amount of water influenced the velocity more than the amount fat (Tellis-Romero et al., 2011).

Attenuation

Attenuation is the loss of energy as the wave travels through a sample. The attenuation takes into account the amplitude of the first and second peak of the ultrasound signal as well as the distance the wave travels. Attenuation is calculated using the following equation:

$$A=A_0e^{-\alpha d}$$

In this equation, A_0 and A refer to the amplitude of the first and second wave, respectively. α is the attenuation coefficient and d is the distance that the wave travels between the two peaks. The

amplitude of the first and second peak can be replaced with the intensity or power of the wave (Pico, 2012).

Energy loss occurs by the absorption and scatterings of the ultrasound wave. Absorption, also referred to as internal attenuation, occurs when an element in the sample absorbs some of the wave's energy (Dukhin et al., 2005). Scattering occurs when pores, holes, or cracks direct the wave away from the transducer. An example of using attenuation for testing a product is the Nassar et al. (2010) study that examined the structure of Cometé cheese at the beginning and end of storage. Before aging, the cheese had a compact structure, which allowed the wave to travel through the sample without experiencing any significant changes. During the aging process, the cheese developed openings and fissures of various sizes, which scattered the ultrasound wave. The size and number of the openings and fissures determined how the wave scattered. A cheese sample with small openings scattered throughout the cheese and no fissures experienced a small change in waveform. As the number of fissures and the size of the openings increased, the waveform began to decrease in size and changed shape. Eventually, the ultrasound signal became lost in the ultrasound noise.

Set-up needed for ultrasound testing

Equipment needed for ultrasound testing

To produce and analyze the ultrasound wave, a pulser-receiver, transducer, oscilloscope, and computer are needed. Wave generation starts with the pulser-receiver. The pulser-receiver determines the voltage/energy of the wave. The energy can be lengthened or dampened. The energy then goes to a piezoelectric transducer, which transforms the energy into a sound wave. After the wave travels through the sample, the transducer converts the sound wave back into energy that returns to the pulser-receiver. The receiver adjusts the energy by amplifying or

increasing the gain and decreases the impedence and noise so the ultrasound wave can be clearly observed. From the pulser-receiver, the energy goes to the oscilloscope for observing the wave. The oscilloscope shows the waveform in an A-scan or B-scan display. In the A-scan, the information is plotted as wave energy vs. time. The B-scan displays the information as the time-of-flight vs the position of the transducer. The waveform is then sent to a computer for further analysis (Pico, 2012).

Methods used for ultrasound testing

The number of transducers determines the type of ultrasound testing. A pulse-echo method uses one transducer and a through-transmission method needs two transducers. Figure 2.1 shows the transfer of the energy and ultrasound wave for a pulse echo and through-transmission method. With the pulse-echo method, one transducer generates and captures the wave. A reflector plate directs the wave back to the transducer. In the through-transmission method, the transducers are placed directly across from one another, and one transducer generates the wave and the other transducer captures the wave (Awad et al., 2012).

Each testing method has its advantages and disadvantages. The pulse-echo method has the simplest set-up and lowest cost (Povey and McClements, 1988; McClements, 1995). With through-transmission, the researcher needs access to opposite sides of a sample. When testing for defects, the through-transmission method detected defects by the intensity of the received wave. In the pulse-echo method, the distance to the defect was estimated. Benedito et al. (2001) conducted tests to determine if a through-transmission or pulse-echo method was better at identifying internal defects in Mahon cheese. When using the through-transmission method, Benedito et al. (2001) mistook small holes that naturally occur in the cheese for internal defects.

For this reason, the through-transmission was not an acceptable method for identifying internal defects in Mahon cheese.

The pulse-echo method proved more successful. The method detected all of the samples that had internal defects. In addition to identifying the internal defect, the researchers estimated the size and distance to the cracks in the cheese. One cheese sample had a crack 1.9 cm away from the surface and the researchers estimated with ultrasound that the crack was between 1.84 cm and 1.98 cm away from the surface. However, the pulse-echo method has difficulty detecting defects that are close to the sample's surface. When the wave is returning to the transducer, the returning wave can get lost in the vibrations from the emitted wave (Pico, 2012). To help the loss of the returning wave, a delay line with known ultrasonic properties can be used to separate incoming and outgoing waves (Coupland, 2004).

Through-transmission tests do not have anything that can alter the production or receiving of the wave. However, through-transmission tests require contact transducers. One limitation of contact transducers is the need for a couplant. Couplants ensure that the environment and air does not alter the ultrasound wave as the wave leaves the transducer and enters the sample. Using a couplant increased preparation time and could contaminate the sample (Cho and Irudayarj, 2003). Without a couplant, inaccurate data will be collected, but studies have been conducted to determine if a specially designed transducer can use air as a couplant. These non-contact transducers can be used during production (Cho and Irudayarj 2003a; Leemans and Destain, 2009). Pallav et al. (2009), Cho and Irudaharj (2003a), and Cho and Irudayarj (2003b) worked with non-contact transducers to detect foreign bodies and determine the mechanical properties of cheese, and found that non-contact transducers can be used. However, non-contact

transducers can be influenced by the environmental factors such as air flow, temperature, and humidity (Cho and Irudayaraj. 2003).

Studies involving ultrasound spectroscopy

One common type of ultrasound testing is ultrasound spectroscopy. With ultrasound spectroscopy, velocity and attenuation values are obtained for a range of frequencies. Velocity can be affected by the frequency. A wave with a lower-frequency is slower than a wave at a higher frequency (Povey and McClements, 1988). With attenuation, increasing the frequency increases the attenuation (Corredig et al., 2004). Also, particles in a sample will absorb or scatter the wave depending on the frequency (Dukhin et al., 2005). The following studies used ultrasound spectroscopy to characterize lactose fluid milk, butter, and dairy powders.

Droplet size determination in milk and butter samples

Ultrasound has the potential to provide information about the composition and structure of a product. An advantage of using ultrasound is the samples do not have to undergo any preparation or other steps that could destroy the sample. Dukhin et al. (2004) used attenuation to determine the fat content and fat droplet size in milk and the water droplet size in butter. The attenuation was compared for commercially available creams, milks, and water. The researchers observed that the attenuation increased as the fat content increased for the milk and butter samples. From the relationship between attenuation and fat content, manufacturers could eventually use attenuation readings to calculate the fat content of a sample and monitor the production of the butter.

Dukhin et al. (2005) collected attenuation values between 1MHz and 100MHz for milk and butter samples. Using milk from the same batch, Dukhin et al. (2005) homogenized part of the milk. The homogenization process led to higher attenuation values. After doing some

calculations, they were able to show the size distribution of the fat or water particles. The fat particle sizes in the homogenized milk were between 0 and 1 μm, and the fat particle sizes in the unhomogenized milk were between 0 and around 100 μm.

Monitoring the dissolution and crystallization of lactose

Saggin and Coupland (2002) and Yucel and Coupland (2010) monitored the dissolution process for lactose powders. Throughout the studies, the two sets of authors noted that a relationship existed between the velocity and dissolved portion of the lactose where the velocity increased as the dissolved portion of lactose increased. After adding the lactose powder, water entered and released the air in the lactose particle, causing the velocity to fluctuate (Yucel and Coupland, 2010). Yucel and Coupland (2010) determined that velocity did not have the ability to monitor the dissolution process, but velocity could monitor the lactose concentration of a solution.

Besides velocity, Saggin and Coupland (2002) tracked the dissolution process by the size of the reflected wave. When the amount of lactose in the solution increased, the reflected wave decreased in size. Like velocity, a linear relationship existed between the reflected wave size and the concentration of lactose in the solution. The researchers used this relationship to determine the amount of lactose in the solution. Yucel and Coupland (2010) collected attenuation data along with velocity data to monitor the dissolution of lactose. Unlike velocity, the concentration of lactose did not influence the attenuation. During dissolution, the attenuation increased and then stabilized. The refractive index monitored the dissolution process off-line and the attenuation results matched those of the refractive index. Studies involving super-saturated solutions noticed an increase in attenuation when the number of lactose crystals in solution increased. The relationship between attenuation and the number of crystals provided information

about the composition of lactose in a solution while the lactose dissolved (Yucel and Coupland, 2010).

The previous studies focused on the dissolution of lactose. Yucel and Coupland (2011) examined the reverse process where the lactose leaves the solution and crystallizes. Like the lactose dissolution studies, this study noticed that the velocity increased as the initial concentration of lactose in the gel increased from 43% to 46%(w/w) During the crystallization process, the velocity unexpectedly decreased. The authors theorized that the decreasing velocity was caused by the lactose crystals scattering the ultrasound waves.

The studies found that attenuation provided more information about changes in lactose than the velocity. When the crystals were forming, ultrasound waves became scattered and the attenuation values increased. Attenuation values also increased as the number of crystals and the concentration of lactose increased. The shape and size of crystals influenced the attenuation values. Turbidity and isothermal calorimetry measurements showed that varying the concentration of lactose led to crystals being formed sooner and the attenuation showed the same trend (Yucel and Coupland, 2011).

Monitoring the dissolution of dairy based powders

Besides lactose, studies have examined the dissolution of other types of dairy based powders. Meyer et al. (2006) conducted experiments on instant milk powder and Richard et al. (2012) conducted experiments on powders that were produced with varying concentrations of native phosphocaseinate, lactose, and whey protein isolate. These two studies compared a reference method to the ultrasound data to determine if ultrasound had the ability to quantify the dissolution behavior and solubility of dairy based powders. Meyer et al. (2006) compared the

ultrasound data to the results of the visual reconstitution test whereas Richard et al. (2012) used a granulomorpheter to visually track the size of the particles.

The visual reconstitution test involved a person scoring the powder on a scale of 0-5 on the amount of undissolved powder after a set period of time. If a powder scored a 0 and had a low score, then no undissolved powder was observed on the surface, and the powder was considered good. Powders with a high score were considered poor dissolving and unacceptable to consumers. After conducting the visual reconstitution test, powders were divided into high, medium, and low scoring powders. Velocity and attenuation data were collected for all the groups and compared to the visual reconstitution test results (Meyer et al., 2006).

Just like the lactose powder, the ultrasound velocity was not able to track the solubility of powder. Meyer et al. (2006) explained that velocity is influenced by the composition of the powders and the composition does not change during dissolution. Therefore, the velocity would not have any significant changes. On the other hand, attenuation was affected by the particle size, which allowed attenuation to characterize the solubility of a powder. When examining the attenuation values, powders that were classified as good had higher attenuation values than the bad powders. After completing all the tests, the researchers concluded that there was a high correlation between the results from the visual reconstitution test and the attenuation values. Powders from another source showed that the test results can be duplicated (Meyer et al., 2006).

Richard et al. (2012) focused on changes in the amplitude of the ultrasound wave as the powders dissolved. Powders containing various proportions of native phosphocaseinate, lactose, and whey protein isolate were created and then tested. The researchers noticed that the amplitude increased and eventually reached an asymptotic value for all of the powders. Whey protein isolate had the shortest time before the signal appeared and before the asymptotic value of the

amplitude was achieved. Powders containing native phosphocaseinate had longer relaxation times, an increased time to reach the asymptotic value for amplitude, and the ultrasound signal appeared later. The increased times are attributed to the water having a difficult time penetrating the powder (Richard et al., 2012).

Richard et al. (2012) observed that for all the powders, the time to reach the asymptotic value was shorter than the rehydration time for all of the powders. They concluded that ultrasound can be used to determine the solubility of the dairy based powders. Another observation involved the extinction of the ultrasound signal once the powder was added. The researchers hypothesized that air bubbles caused the extinction of the signal. One theory was the stirring condition or surface air caused the bubbles. Additional experiments showed that the solvent forced the air out of the powder particles and created the bubbles in the solution. A similar result was mentioned earlier when Yucel and Coupland (2010) attributed the fluctuating velocity to air leaving the lactose powder.

Monitoring the coagulation of milk

Alternative to the heat stability test

Another type of test that can be replaced is the heat stability test. Lehmann and Buckin (2005) conducted an experiment to determine if ultrasound spectroscopy could replace the Irish Dairy Board method and the Standard Association of Australia method for determining the heat stability of milk and milk products. These two methods rely on human judgement. When observing the samples with ultrasound, four stages were identified for the ultrasound velocity difference. The ultrasound velocity difference involved subtracting a reference value from the absolute ultrasonic velocity. Each stage correlated the physical change in the sample with the velocity readings. In the first 300 s of testing, velocity quickly decreased. The denaturation of

whey, calcium leaving the micelle, and the sample adjusting to higher temperatures caused a reduction in velocity. From 300-850 s, the sample entered the pre-coagulation stage, where the velocity decreased at a slower rate. The rate of change varied depending on the nature and pH of the sample. The third stage lasted from 800-1100 s. The casein micelles began to aggregate and caused the velocity to decrease at a quicker rate. After 1100 s, the velocity experienced little change since the coagulation period had ended.

When examining the attenuation, the casein size and the nature of the sample influenced the attenuation values. As the size of the casein micelles increased, the attenuation values began to increase as well. For all the samples, the end of coagulation was determined when the attenuation suddenly decreased. The author suggested the velocity and attenuation should be monitored at the same time to fully understand the coagulation process. This is especially true for fast-coagulating samples. With fast-coagulating samples, the velocity may not detect coagulation as the sample adjusts to the temperature, but the attenuation would be able to provide information about the size of the proteins. The authors concluded that ultrasound spectroscopy can be an instrument for determining the heat stability of milk and milk products.

Monitoring acid coagulation

Instead of heat, producers have used acid and rennet to coagulate milk. Fermented dairy products such as yogurt are produced by acid coagulation. Glucano-δ-lactone (GDL) and lactic acid bacteria lower the pH of the milk samples. Dalgleish, Alexander and Corredig (2004), Corredig et al. (2004), and Gulseren, Alexander, and Corredig (2010) examined the acid coagulation of heated and unheated milk samples. They noticed that the heated milk samples had higher attenuation values. Gulseren et al. (2010) explained that the aggregation of whey proteins in the heated milk samples led to higher attenuation values. Corredig et al. (2004) noticed that

the velocity gradient for heated milk contained a brief stabilization period at a pH of 5.3. This stabilization period was attributed to the start of gelation. With the unheated milk samples, a peak was noticed at the pH of 5 when gelation starts. The other two studies did not have a peak in their velocity graphs. Corredig et al. (2010) and Dalgleish et al. (2010) mentioned that heated milk samples produce a more elastic and stronger gel, but the ultrasound data did not detect the gel strength differences between the heated and unheated samples.

Krasaekoopt, Bhandari and Deeth (2004) conducted an experiment to compare data from a rapid visco analyzer (RVA) and velocity. They found that velocity could detect changes in the sample's viscosity before the RVA. At the beginning of fermentation, velocity varied and started to increase when the sample began to form a gel. Since the study was conducted with lactic acid bacteria, the ultrasound had the capability of detecting the formation of lactic acid and the aggregation of the casein micelles.

Dalgleish et al. (2004), Corredig et al. (2004), and Dalgleish, Verespej, Alexander and Corredig (2005) agreed that the velocity increased throughout the acidification process. All of the studies explained that the increase in velocity happens during the dissolution of the calcium from the micelle to the serum. After addition of GDL, the velocity increased (Dalgleish et al., 2005). Throughout the acidification process, the velocity increased at a slow and then a fast rate. Eventually, the velocity readings stabilized (Dalgleish et al., 2004). Dalgleish et al. (2005) added that a small portion of the velocity change cannot be explained by the dissolution of calcium.

Dalgleish et al. (2004), Dalgleigh et al. (2005), and Gulseren et al. (2010) found dissolution of calcium affected the attenuation values. Dalgelish et al. (2004) noticed that the attenuation increased as the pH decreased and eventually the attenuation readings stabilized. The authors noticed that the attenuation increased at a faster rate than velocity. Dalgleish et al. (2005)

found a linear relationship between the calcium in the serum and the attenuation and noted that the casein and serum protein scatter the wave.

Monitoring rennet coagulation

The last way to coagulate milk is to use rennet. Corredig et al. (2004) monitored the rennet-induced coagulation of milk with ultrasound spectroscopy. Corredig et al. (2004) monitored the velocity and attenuation as the rennet coagulation occurred. The researchers reduced the concentration of rennet that was added to the milk so that they could better observe the changes in velocity and attenuation. The study tested to see if the rennet concentration affected the ultrasound data. They found that the ultrasound data had the same trend, but the higher concentration had a shorter lag time at the beginning of an experiment. When the rennet concentration increased, the casein bonds were cleaved at a faster rate and the para-κ-casein began to aggregate sooner. Since the milk changed at a faster rate, the ultrasound data changed at a similar rate (Corredig et al., 2004).

Corredig et al. (2004) noticed that the velocity decreased, increased, and then increased at a slower rate. Eventually, the velocity stabilized towards the end. Four or five hours after the rennet addition, syneresis started to occur and the velocity began to increase again. The slow and fast rate of change for the velocity was related to the different steps in the coagulation process. A slow rate of change occurred when the enzyme was cleaving the 104-105 peptide bond of the κ-casein to produce the para-κ-casein and the glycomacropeptide. The glycomacropepetide dissolved into the whey and the para-κ-casein began to aggregate. During the aggregation process, the velocity increased at a faster. Some slight changes in velocity were attributed to the natural variation of milk samples.

Corredig et al. (2004) found that attenuation was more sensitive to changes in the milk sample. Corredig et al. (2004) observed that the attenuation reached a maximum point 10 minutes before the velocity. During the renneting process, the attenuation quickly increased and then decreased (Corredig et al., 2004). Corredig et al. (2004) explained how the attenuation changed during the coagulation process. The attenuation did not show much change in the beginning because the casein was not aggregating. As the para-κ- casein began to aggregate and grow in size, the attenuation values increased. During this time, the elasticity of the sample did not change. Later on, velocity became more sensitive to the sample's properties because gelling and elasticity changed and not the size of the protein.

Future research

When examining the literature, low-intensity ultrasound proves to be useful for testing characteristics and composition of various dairy products. However, only four studies focused on using ultrasound to examine the solubility of dairy-based powders. Solubility of the powder is important to the food industry. During processing, insoluble powders can clog filters or create a sedimentation layer. If the appropriate amount of powder does not reach the final product, then the protein content and functional properties such as water binding ability will be lost (Cooredig, 2009; Chandan & Kilra, 2011).Further research can be done on quantifying the solubility of commercially available MPC, WPC, or other high-protein dairy powders. The research articles did not provide an ultrasonic testing method that could be used for all types of powder.

A commonality between all of the studies is the use of ultrasound spectroscopy. The equipment for ultrasound spectroscopy can be expensive and requires skilled technicians. Therefore, cheaper ultrasound equipment could be tested with dairy powders, cheese, milk, or other products so that commercial manufacturers can rapidly test their products. With dairy

powders, an ultrasonic flaw detector can be used to test the solubility of the powder. Ultrasonic flaw detectors are commonly used in the construction industry and are a fraction of the cost of the equipment needed for ultrasound spectroscopy. The ultrasonic flaw detector has all the needed equipment in one portable device.

Conclusions

MPC and WPC are added to various food products, but the solubility of the product can limit the use of the product. MPC loses solubility during storage as the time and temperature increases. The loss in solubility is attributed to changes that occur with the casein. Micelle-micelle interactions limit the ability of water to disintegrate the particle. Minerals such as calcium, magnesium, and phosphorus also limit solubility. Solubility can be increased by increasing the amount of whey protein or sodium, or by changing the dissolution conditions. Increasing stirring speed and dissolution temperature as well as changing the dissolution liquid can improve the solubility. Whey proteins, on the other hand, do not experience significant changes in solubility during storage. However, WPC powders can become unstable when added at high temperature. So, manufacturers are developing heat-stable WPC powders by reducing the size of particles and adding sugar to WPC. With solubility being an important characteristic for powders, several solubility tests are available. However, they can be subjective, time-consuming, difficult to reproduce, or may require expensive equipment. The use of ultrasound proves to be a potential new method. Ultrasound spectroscopy has successfully characterized several dairy foods products. However, ultrasound spectroscopy can be expensive, but research can be conducted to determine if an ultrasonic flaw detector can characterize the solubility of high-protein dairy powders.

Table 2-2 Methods for solubility testing of high-protein dairy powders

Reference	Equipment	Summary of method	Feasibility
Anema et al., 2006	Solubility test (oven drying)	5% concentration of powder added to water and maintained at 30°C for thirty minutes. Sample removed, centrifuged at 700 x g for 10 minutes. The totals solids were calculated for the supernatant	Time-consuming Quantify solubility
Gaini et al., 2006	Rheometer	A specially designed four blade stirrer was used with a C25 cup. The shear rate was set at $100s^{-1}$. When the rheometer had ran for 50s, powder was added to 18ml of water. Data was collected every 20s for the first 5000s and then every 1000s.	Skilled Technician Little to no sample preparation
Gaiani et al., 2009	Turbidity sensor	A 2 L vessel was used and an overhead stirrer was set at 400 rpm. The temperature was kept at 24 °C. The turbidity sensor was located 3 cm below the surface of the water and the stirrer did not interfere with the sensor. The light was 860 nm and the incident beam reflected back at 180°.Data was collected every second for 100s and then every 5 s. The total experiment time was 50,000 s.	Time-consuming Little to no sample preparation
Mimouini et al., 2009	Static light scattering	A 4ml sample of 5% (w/w) concentration of powder solution was added to 800 mL of 20 °C distilled water that was circulating at 2000 rpm. After 1 minute, the light scattering pattern was obtained. Data was collected at regulation intervals for 210 min.	Expensive Equipment Rapid Reproducible
Fang et al., 2011	FBRM	Approximately 7.5 g MPC was added to 500ml distilled water and stirred at 800rpm. The FBRM collected data every 10s for 30min. The counts for <10 μm, 10-50 μm, 50-150 μm, 150-300 μm were examined.	Expensive Equipment Little to no sample preparation Quantify solubility

Reference	Equipment	Summary of method	Feasibility
Richard et al., 2012	Ultrasound spectroscopy	Two 1MHZ transducers were placed 2 cm apart. To 1 L of solvent, 2 g of powder were added and a magnetic stirrer was set 450 rpm. The solution temperature was maintained at 30 °C. The amplitude of the ultrasound wave was used to calculate attenuation.	Expensive Equipment Skilled Technician
Schuck et al., 2002	Nuclear magnetic resonance (NMR)	To 20 g of water, 1 g of powder was added and a stirrer was set at 1100 rpm.Tests were performed at 40 °C at a resonance frequency of 10MHz. During the reconstitution a decay curve was obtained using a maximum of 845 spins every 20 s. The interpulse space between 180° pulses was 2 ms.	Expensive Equipment Skilled Technician Use with other method to determine solubility Quantify solubility
Crowley et al., 2015	Analytical centrifuge	The intensity of NIR light was measured. MPC was rehydrated for 90 min and 24 h. 400 µl of MPC was added. The samples were centrifuged at 36 x g for 10min and then centrifuged at 168 x g for 10 min. Data was collected at 10 s and then at regular intervals for 20 min. Sediment height was then calculated.	Expensive Equipment Time-consuming Little to no sample preparation Quantify solubility

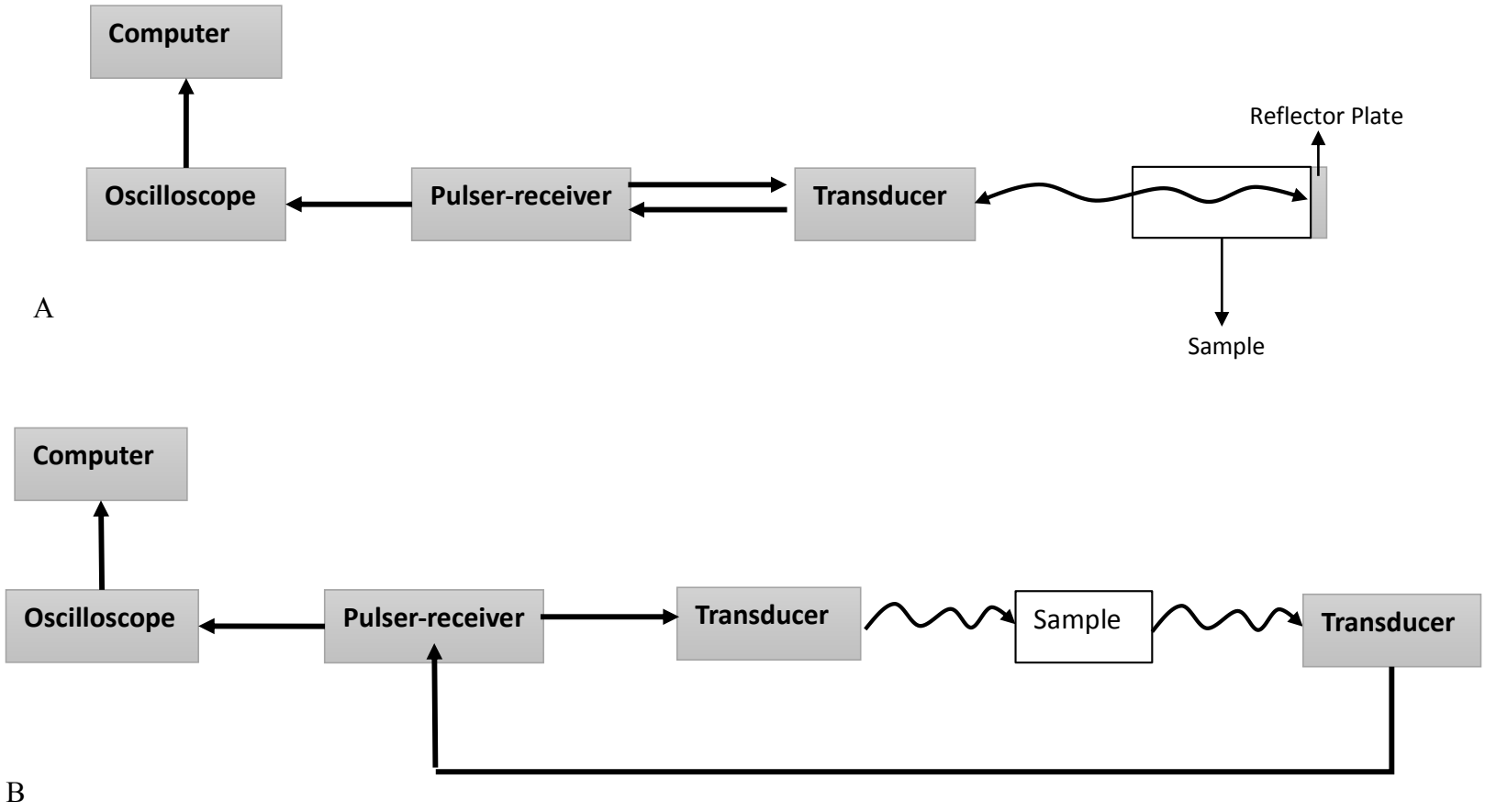

Figure 2-1 Transfer of energy and wave for the pulse-echo method (A) and through-transmission method (B)

References

Abd El-Salam, M. H., S. El-Shibiny and A. Salem. 2009. Factors affecting the functional properties of whey protein products: A review. Food Rev. Int. 25:251-270.

Agarwal, S., R. L. W. Beausire, S. Patel and H. Patel. 2015. Innovative uses of milk protein concentrates in product development. J. Food Sci. 80:A23-A29.

Anema, S. G., D. N. Pinder, R. J. Hunter and Y. Hemar. 2006. Effects of storage temperature on the solubility of milk protein concentrate (MPC85). Food Hydrocoll. 20:386-393.

Ashokkumar, M., J. Lee, B. Zisu, R. Bhaskarcharya, M. Palmer and S. Kentish. 2009. Hot topic: Sonication increases the heat stability of whey proteins. J. Dairy Sci. 92:5353-5356.

Awad, T. S., H. A. Moharram, O. E. Shaltout, D. Asker and M. M. Youssef. 2012. Applications of ultrasound in analysis, processing and quality control of food: A review. Food Res. Int. 48:410-427.

Benedito, J., J. Carcel, G. Clemente and A. Mulet. 2000. Cheese maturity assessment using ultrasonics. J. Dairy Sci. 83:248-254.

Benedito, J., J. Carcel, M. Gisbert and A. Mulet. 2001. Quality control of cheese maturation and defects using ultrasonics. J. Food Sci. 66:100-104.

Cakir-Fuller, E. 2015. Enhanced heat stability of high protein emulsion systems provided by microparticulated whey proteins. Food Hydrocoll. 47:41.

Chandan, R. C. and A. Kilara. 2011. Dairy Ingredients for Food Processing. Amex, Iowa: Wiley- Blackwell, Amex, Iowa.

Chandrapala, J., C. Oliver, S. Kentish and M. Ashokkumar. 2012. Ultrasonics in food processing - food quality assurance and food safety. Trends Food Sci. Technol. 26:88-98.

Cho, B. and J. M. K. Irudayaraj. 2003. Foreign object and internal disorder detection in food materials using noncontact ultrasound imaging. J. Food Sci. 68:967-974.

Cho, B. and J. M. K. Irudayaraj. 2003. A noncontact ultrasound approach for mechanical property determination of cheeses. J. Food Sci. 68:2243-2247.

Corredig, M., M. Alexander and D. G. Dalgleish. 2004. The application of ultrasonic spectroscopy to the study of the gelation of milk components. Food Res. Int. 37:557-565.

Coupland, J. N. 2004. Low intensity ultrasound. Food Res. Int. 37:537-543.

Crowley, S. V., B. Desautel, I. Gazi, A. L. Kelly, T. Huppertz and J. A. O'mahony. 2015. Rehydration characteristics of milk protein concentrate powders. J. Food Eng. 149:105-113.

Dalgleish, D., M. Alexander and M. Corredig. 2004. Studies of the acid gelation of milk using ultrasonic spectroscopy and diffusing wave spectroscopy. Food Hydrocoll. 18:747-755.

Dalgleish, D. G., E. Verespej, M. Alexander and M. Corredig. 2005. The ultrasonic properties of skim milk related to the release of calcium from casein micelles during acidification. Int. Dairy J. 15:1105-1112.

Dukhin, A. S., P. J. Goetz and B. Travers. 2005. Use of ultrasound for characterizing dairy products. J. Dairy Sci. 88:1320-1334.

Fang, Y., S. Rogers, C. Selomulya and X. Chen. 2012. Functionality of milk protein concentrate: Effect of spray drying temperature. Biochem. Eng. J. 62:101-105.

Fang, Y., C. Selomulya, S. Ainsworth, M. Palmer and X. D. Chen. 2011. On quantifying the dissolution behaviour of milk protein concentrate. Food Hydrocoll. 25:503-510.

Fang, Y., C. Selomulya and X. Chen. 2010. Characterization of milk protein concentrate solubility using focused beam reflectance measurement. Dairy Science & Technology; Dairy Sci.Technol. 90:253-270.

Fang, Y., C. Selomulya and X. Chen. 2008. On measurement of food powder reconstitution properties. Drying Technol. 26:3-14.

Food and Drug Administration (FDA). 2014. Agency response letter GRAS notice no. GRN 000503. Accessed Aug. 20, 2015. http://www.fda.gov/Food/ IngredientsPackagingLabeling/GRAS/NoticeInventory/ucm427497.htm

Fyfe, K. N., O. Kravchuk, T. Le, H. C. Deeth, A. V. Nguyen and B. Bhandari. 2011. Storage induced changes to high protein powders: Influence on surface properties and solubility. J. Sci. Food Agric. 91:2566-2575.

Gaiani, C., J. J. Ehrhardt, J. Scher, J. Hardy, S. Desobry and S. Banon. 2006. Surface composition of dairy powders observed by X-ray photoelectron spectroscopy and effects on their rehydration properties. Colloids and Surfaces B: Biointerfaces. 49:71-78.

Gaiani, C., J. Scher, P. Schuck, J. Hardy, S. Desobry and S. Banon. 2006. The dissolution behaviour of native phosphocaseinate as a function of concentration and temperature using a rheological approach. Int. Dairy J. 16:1427-1434.

Gaiani, C., J. Scher, P. Schuck, S. Desobry and S. Banon. 2009. Use of a turbidity sensor to determine dairy powder rehydration properties. Powder Technol. 190:2-5.

Gaiani, C., P. Schuck, J. Scher, S. Desobry and S. Banon. 2007. Dairy powder rehydration: Influence of protein state, incorporation mode, and agglomeration. J. Dairy Sci. 90:570-581.

Gazi, I. and T. Huppertz. 2015. Influence of protein content and storage conditions on the solubility of caseins and whey proteins in milk protein concentrates. Int. Dairy J. 46:22-30.

Gulseren, I., M. Alexander and M. Corredig. 2010. Probing the colloidal properties of skim milk using acoustic and electroacoustic spectroscopy. effect of concentration, heating and acidification. J. Colloid Interface Sci. 351:493-500.

Hsu, K. and O. Fennema. 1989. Changes in the functionality of dry whey protein concentrate during storage. J. Dairy Sci. 72:829-837.

Jeantet, R., P. Schuck, T. Six, C. Andre and G. Delaplace. 2010. The influence of stirring speed, temperature and solid concentration on the rehydration time of micellar casein powder. Dairy Science & Technology; Dairy Sci.Technol. 90:225-236.

Krasaekoopt, W., B. Bhandari and H. Deeth. 2005. Comparison of gelation profile of yoghurts during fermentation measured by RVA and ultrasonic spectroscopy. Int. J. Food Prop. 8:193-198.

Koh, L., J. Chandrapala, B. Zisu, G. Martin, S. Kentish and M. Ashokkumar. 2014. A comparison of the effectiveness of sonication, high shear mixing and homogenisation on improving the heat stability of whey protein solutions. Food Bioprocess Technol. 7:556-566.

Kulmyrzaev, A., C. Bryant and D. J. Mcclements. 2000. Influence of sucrose on the thermal denaturation, gelation, and emulsion stabilization of whey proteins. J. Agric. Food Chem. 48:1593.

Liu, G. and Q. Zhong. 2015. High temperature- short time glycation to improve heat stability of whey protein and reduce color formation. Food Hydrocoll. 44:453-460.

Leemans, V. and M. Destain. 2009. Ultrasonic internal defect detection in cheese. J. Food Eng. 90:333-340.

Lehmann, L. and V. Buckin. 2005. Determination of the heat stability profiles of concentrated milk and milk ingredients using high resolution ultrasonic spectroscopy. J. Dairy Sci. 88:3121-3129.

McClements, D. J. 1995. Chapter 4 - ultrasonic characterization of foods. Pages 93-116 in Characterization of Food. A. G. Gaonkar ed. Elsevier Science B.V., Amsterdam.

Meyer, S., V. S. Rajendram and M. J. W. Povey. 2006. Characterization of reconstituted milk powder by ultrasound spectroscopy. J. Food Qual. 29:405-418.

Mimouni, A., H. C. Deeth, A. K. Whittaker, M. J. Gidley and B. R. Bhandari. 2009. Rehydration process of milk protein concentrate powder monitored by static light scattering. Food Hydrocoll. 23:1958-1965.

Mimouni, A., H. C. Deeth, A. Whittaker, M. Gidley and B. Bhandari. 2010a. Investigation of the microstructure of milk protein concentrate powders during rehydration: Alterations during storage. J. Dairy Sci. 93:463-472.

Mimouni, A., H. C. Deeth, A. K. Whittaker, M. J. Gidley and B. R. Bhandari. 2010b. Rehydration of high-protein-containing dairy powder: Slow- and fast-dissolving components and storage effects. Dairy Science & Technology. 90:335-344.

Mulet, A., J. Benedito, J. Bon and C. Rossello. 1999. Ultrasonic velocity in cheddar cheese as affected by temperature. J. Food Sci. 64:1038-1041.

Nassar, G., F. Lefbvre, A. Skaf, J. Carlier, B. Nongaillard and Y. Noêl. 2010. Ultrasonic and acoustic investigation of cheese matrix at the beginning and the end of ripening period. J. Food Eng. 96:1-13.

Pallav, P., D. A. Hutchins and T. H. Gan. 2009. Air-coupled ultrasonic evaluation of food materials. Ultrasonics. 49:244-253.

Pelegrine, D. H. G. and C. A. Gasparetto. 2005. Whey proteins solubility as function of temperature and pH. LWT - Food Science and Technology. 38:77-80.

Pelegrine, D. H. G. and M. T. M. S. Gomes. 2012. Analysis of whey proteins solubility at high temperatures. International Journal of Food Engineering. 8:1-8.

Pico, Y. 2012. Chapter 5 - low-intensity ultrasounds. Pages 117-144 in Chemical Analysis of Food: Techniques and Applications. Y. Picó ed. Academic Press, Boston.

Povey, M. J. W. and D. J. McClements. 1988. Ultrasonics in food engineering. part I: Introduction and experimental methods. J. Food Eng. 8:217-245.

Povey, M. J. W. 1989. Ultrasonics in food engineering part II: Applications. J. Food Eng. 9:1-20.

Rich, L. M. and E. A. Foegeding. 2000. Effects of sugars on whey protein isolate gelation. J. Agric. Food Chem. 48:5046.

Richard, B., J. F. Le Page, P. Schuck, C. Andre, R. Jeantet and G. Delaplace. 2013. Towards a better control of dairy powder rehydration processes. Int. Dairy J. 31:18-28.

Richard, B., M. Toubal, J. Le Page, G. Nassar, E. Radziszewski, B. Nongaillard, P. Debreyne, P. Schuck, R. Jeantet and G. Delaplace. 2012. Ultrasound tests in a stirred vessel to evaluate the reconstitution ability of dairy powders. Innovative Food Science & Emerging Technologies. 16:233-242.

Saggin, R. and J. N. Coupland. 2002. Ultrasonic monitoring of powder dissolution. J. Food Sci. 67:1473-1477.

Schuck, P., A. Davenel, F. Mariette, V. Briard, S. Méjean and M. Piot. 2002. Rehydration of casein powders: Effects of added mineral salts and salt addition methods on water transfer. Int. Dairy J. 12:51-57.

Schuck, P., S. Mejean, A. Dolivet, C. Gaiani, S. Banon, J. Scher and R. Jeantet. 2007. Water transfer during rehydration of micellar casein powders. Lait; Lait. 87:425-432.

Sikand, V., P. S. Tong, S. Roy, L. Rodriguez-Saona and B. A. Murray. 2011. Solubility of commercial milk protein concentrates and milk protein isolates. J. Dairy Sci. 94:6194-6202.

Telis-Romero, J., H. A. Vaquiro, J. Bon and J. Benedito. 2011. Ultrasonic assessment of fresh cheese composition. J. Food Eng. 103:137-146.

Yucel, U. and J. N. Coupland. 2011. Ultrasonic characterization of lactose crystallization in gelatin gels. J. Food Sci. 76:E48-E54.

Yucel, U. and J. N. Coupland. 2010. Ultrasonic characterization of lactose dissolution. J. Food Eng. 98:28-33.

Chapter 3 - Research objectives

This study focused on developing and evaluating an ultrasonic flaw detector based method to determine the solubility of high-protein dairy powders. Another focus of the study was to study the effect of protein content and dissolution temperature on the solubility of high-protein dairy powders. The specific objectives for the study are located below:

1. To determine the optimal settings for an ultrasonic flaw detector to characterize the solubility of high-protein dairy powders
2. To determine if the proposed ultrasonic flaw detector-based method can characterize the solubility of MPC80 that has been stored at different temperatures.
3. To use the proposed ultrasonic flaw detector method to determine how the protein content effects the solubility of MPC and MPI powders
4. To use the proposed ultrasonic flaw detector to determine how the dissolution temperature effects the solubility of MPC and MPI powders

Chapter 4 - Development of a method to characterize high-protein dairy powders using an ultrasonic flaw detector[1]

Abstract

Dissolution behavior of high-protein dairy powders plays a critical role for achieving functional and nutritional characteristics of a finished food product. Current methods for evaluating powder dissolution properties are time consuming, difficult to reproduce, and subjective. Ultrasound spectroscopy is a rapid and precise method, but requires expensive equipment and skilled technicians to carry out the tests. In the present study, an ultrasonic flaw detector (UFD) was used as an economical alternative to characterize the powder dissolution properties. The objective of study was to develop a method to characterize the dissolution behavior of MPC using an UFD. The experimental setup included an UFD connected to a 1MHz immersion transducer that was kept a constant distance from a reflector plate. To validate the method, two batches of MPC80 from a commercial manufacturer were procured and stored at 25 °C and 40 °C for 4 weeks. Focus beam reflectance measurement (FBRM) and solubility index were used as reference methods. Relative ultrasound velocity and ultrasound attenuation were acquired during the dissolution of MPC samples. In order to characterize the MPC dissolution, 4 parameters including standard deviation of relative velocity, area under the attenuation curve, and peak attenuation were extracted from ultrasound data. As the storage temperature and time increased, the area under the attenuation curve and peak height decreased, indicating a loss of solubility. The proposed UFD-based method was able to capture the changes in dissolution of MPC during storage at 25 °C and 40 °C. It was observed that a high-quality MPC had a low

[1] Accepted for publication: Journal of Dairy Science

standard deviation and a larger area under the attenuation curve. As the MPC aged at 40 °C, the particle dispersion rate decreased and consequently an increase in standard deviation and reduction in area were observed. Overall, the UFD can be a low-cost method to characterize the dissolution behavior of high-protein dairy powders.

Keywords: ultrasonic flaw detector, milk protein concentrate, solubility

Introduction

When choosing a high-protein dairy powder such as milk protein concentrate (MPC) or milk protein isolate (MPI), dissolution behavior is an important property to consider. High-protein content in MPC yields a powder that is typically less soluble than skim milk powder (Chandan and Kilra, 2011). Nutritional drinks, fermented dairy drinks, and various other food products utilize MPC to improve nutritional and functional properties. A slowly dissolving powder can complicate production by clogging filters and forming a sedimentation layer (Corredig, 2009; Chandan and Kilra, 2011). Consequently, the finished product may not have the intended nutritional and functional characteristics such as protein content and water holding capacity, respectively.

The solubility of MPC is affected by intrinsic and extrinsic parameters such as protein content, dissolution temperature, and storage conditions. Below ambient temperatures and at a low relative humidity, MPC can be stored for up to 6 to 8 months without adversely affecting the solubility. However, storage temperatures above 40 °C drastically reduce the solubility of high-protein MPC powders (Agarwal et al., 2015). Current methods for evaluating dissolution characteristics of powders include the Baumann method (Wallingford and Labuza, 1983), filtration/centrifugation tests (Kneifel et al., 1991), and paste-water retention (Quinn and Paton, 1979). Anema et al. (2006) utilized solubility index as a method to study the effect of storage

temperature on the solubility of MPC. These methods are time consuming, lack precision, and difficult to reproduce. A possible alternative is to use ultrasound spectroscopy as a tool to monitor powder dissolution properties (Fang et al., 2008).

Ultrasound is defined as sound waves that have a frequency above the human hearing of 20kHz. Low-intensity ultrasound has a power below 1 W/cm^2 and a frequency above 100 kHz (Pico, 2012). Low-intensity ultrasound based techniques have the advantage of being rapid, precise, and non-destructive (Dolatowski et al., 2007). In dairy foods applications, low-intensity ultrasound has successfully been used to monitor rennet coagulation (Gunasekaran and Ay, 1996; Corredig et al., 2004) and to identify internal defects and foreign objects in cheese (Leemans and Destain, 2009; Nassar et al., 2010). Through-transmission and pulse-echo modes are used in ultrasound based techniques for evaluating quality of food products. However, McClements (1995) supported the pulse-echo mode as it is easy to design and operate, and is automated. Moreover, Povey and McClements (1988) stated that a pulse-echo method has the lowest cost for ultrasonic testing. Richard et al. (2012) demonstrated that ultrasound spectroscopy in a through-transmission mode can monitor the interactions between the dairy-based powders and solvents, and can be correlated to the powder's solubility. Meyer et al. (2006) also used an ultrasound spectrometer in pulse-echo mode to correlate the attenuation coefficient, an ultrasound spectroscopy parameter, with the visual reconstitution test for instant milk powder.

The literature provides evidence that the ultrasound spectroscopy can be a valuable tool in characterizing powder dissolution properties. Expensive instrumentation and the need for skilled technicians to perform tests keep the ultrasound spectroscopy from being widely used in the dairy industry for routine testing of dairy powders. A commercially available and portable ultrasonic flaw detector (UFD) provides an economical alternative to ultrasound spectroscopy.

An UFD costs around $5,000, which is a fraction of the cost of an ultrasound spectrometer. UFDs are commonly used in the construction industry to detect flaws and cracks in welds, metal, and structures (Olympus, 2007).

The objective of this study was to develop and validate a new UFD-based rapid method to characterize the dissolution behavior of high-protein dairy powders. This study was focused on developing and evaluating the proposed method using MPC80 as a model system.

Materials and methods

Experimental design

MPC80 was used as a model system for the development and evaluation of the proposed method. Initially, UFD parameters such as powder concentration, stirring method, ultrasound path length (distance between the reflector plate and transducer), damp, and energy were optimized in order to increase the signal to noise ratio and also to collect as much ultrasound data as possible. To evaluate the method, 2 batches of commercially available MPC80 were procured and stored for up to 4 weeks at 25 °C and 40 °C to produce powders with different dissolution characteristics. The dissolution characteristics of powders were measured using the proposed UFD-based method as well as using a focused beam reflectance measurement (FBRM) technique and solubility index as reference methods.

Experimental setup

Figure 4.1A shows the experimental setup consisting of an UFD (Epoch LTC, Olympus Scientific Solutions, Waltham, MA), FBRM (Particle Track E25, Mettler Toldeo, Columbus, OH), an immersion transducer (V303-SU; Olympus Scientific Solutions, Waltham, MA), a purpose-build transducer holder, and a four-laded overhead stirrer (Caframo, Georgian Bluffs, Ontario, Canada) that was placed 10 mm from the bottom of the beaker. A temperature

controlled water bath (Fisher Scientific, Pittsburgh, PA) maintained the powder dissolution temperature at 40±0.1 °C.

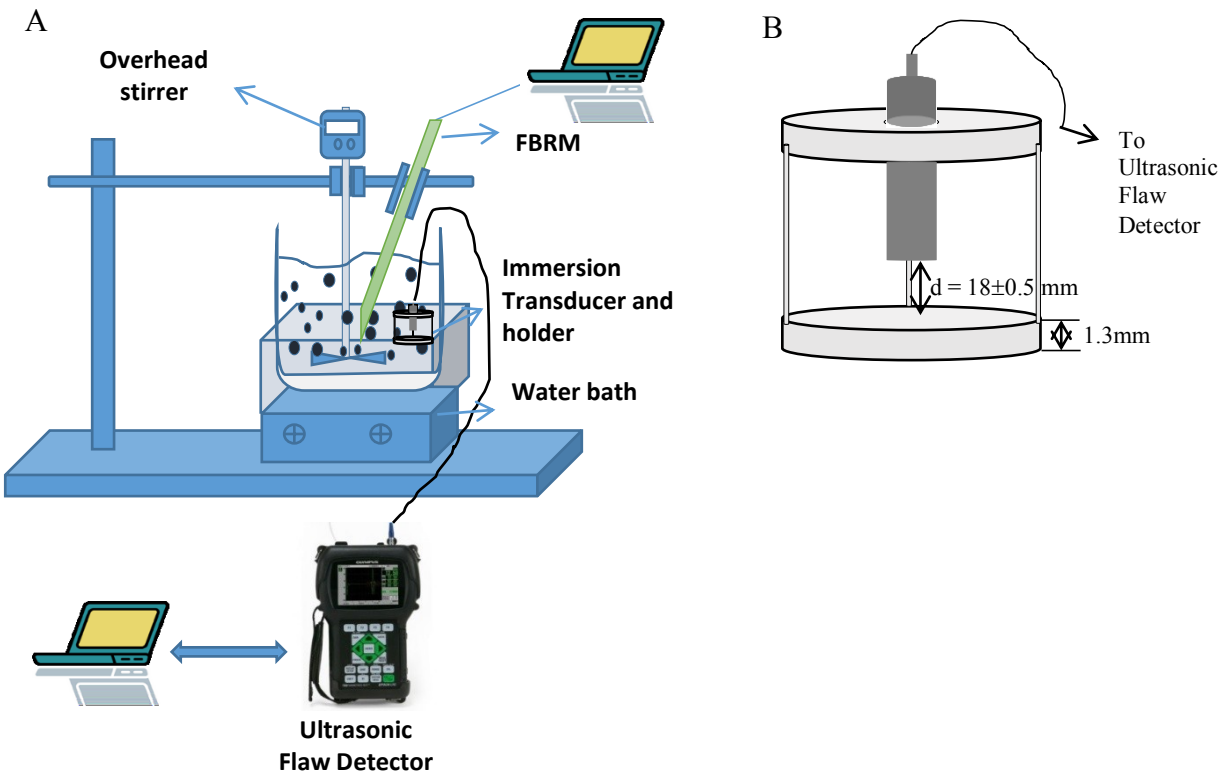

Figure 4-1 (A) Experimental setup used for characterizing powder dissolution; (B) Immersion transducer holder

Ultrasonic flaw detector (UFD)

An UFD in pulse-echo mode was connected to a 1 MHz immersion transducer as shown in Figure 4.1A. A stainless steel holder (Figure 4.1B) was fabricated at a local machine shop to hold the ultrasonic transducer and also to keep the ultrasound path length constant throughout an experiment. The holder consisted of a top and a bottom plate with a diameter of 48.34 mm and thickness of 1.3 mm. The top and bottom plates were placed in such a way that the ultrasound signal traveled through the medium, reflected off the bottom plate, and returned to the transducer. Before adding powder, the stirrer was set at 400 rpm and ultrasound data was collected for water at 40 °C as a baseline.

FBRM

A FBRM was used as a reference method to monitor the dissolution of powder. The FBRM was set at a 30° angle to the vertical axis and 20 mm from the bottom of the beaker. Data from the FBRM was acquired with the icFBRM 4.3 (Mettler Toledo, Columbus, OH) program and counted the number of particles in the following categories: <10 µm, 10-50 µm, 50-150 µm, 300-1000 µm. The change in particle counts was used to monitor the dissolution characteristics of MPC. In this study, only particles between 10 µm and 150µm were considered.

Optimization of UFD-based method parameters

Preliminary studies were carried out using MPC80 as a model system to determine the optimum settings including: powder concentration (2.5%, 5%, 7.5%, and 10% (w/w)), stirring speed (400 - 900 rpm), path length (17.5 – 50 mm), damp (50 – 400 ohms), and energy (100 – 400 Volts).

Deriving parameters from UFD

Figure 4.2 shows a typical ultrasound signal with the amplitude for the first (A_0) and second echo (A). The time-of-flight and amplitude data were exported from GageView Pro (Olympus Scientfic Solutions, Waltham, MA) to Microsoft Excel (Microsoft Seattle, WA) and used to calculate the ultrasound velocity and attenuation. Ultrasound velocity (V) was calculated using Equation 1, where d is the distance between the transducer and the bottom reflector plate, and t is time-of-flight, the time taken for the ultrasound wave to travel a distance of 2d.

$$V\left(\frac{m}{s}\right) = \frac{2d}{t} \qquad (1)$$

From the ultrasound velocity, relative ultrasound velocity was calculated as a ratio of ultrasound velocity of the solution containing powder to that of distilled water at 40 °C. The

ultrasound attenuation (α) was calculated using Equation 2, where A_0 and A represent the ultrasound amplitude for the first and second echo, respectively.

$$\alpha\ (\text{Neper/mm}) = \frac{\ln\left(\frac{A_0}{A}\right)}{2d} \qquad (2)$$

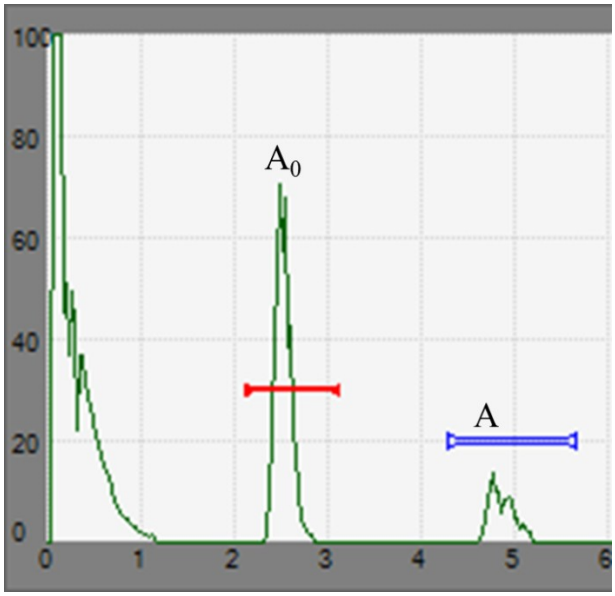

Figure 4-2 Typical ultrasonic flaw detector signal with the first (A_0) and second peak (A)

Relative ultrasound velocity and attenuation were plotted against powder dissolution time. From these curves, the standard deviation of relative ultrasound velocity from 900 -1800 s, attenuation peak height (maximum attenuation), attenuation peak time (time to reach maximum attenuation), and area under the attenuation curve were extracted to characterize powder dissolution. The area under the attenuation curve was calculated using the trapezoidal rule. The derived ultrasound parameters were compared to the results obtained from the FBRM and solubility index to evaluate the relationship between the dissolution characteristics of the powder and the derived ultrasound parameters.

Solubility index

The solubility index was carried out following the method described by Anema et al. (2006). A 15 mL sample was taken at 30 minutes and centrifuged at 700 x g for 10 minutes using a centrifuge (Fisher Scientific, Pittsburgh, PA). The total solids in the supernatant were determined using the standard method (Anema et al., 2006). The soluble material, σ, was calculated using Equation 3.

$$\sigma = \frac{weight\ of\ dry\ material}{weight\ of\ solution} x100\% \qquad (3)$$

Evaluation of UFD-based method

To evaluate the method, two batches of MPC80 from a commercial manufacturer were procured and stored at 25 °C and 40 °C for 4 weeks. The composition of MPC80, obtained from the manufacturer, was approximately 80.4% protein, 5.5% moisture, 6.6% ash, 1.1% fat, and 6.4% lactose. The dissolution characteristics of the samples were evaluated on Day 0, Day 3, Week 1, Week 2, Week 3, and Week 4. Day 0 powder was referred to as fresh powder. On each experimental day, dissolution properties of MPC were characterized using the UFD, FBRM, and solubility index. In a 1L beaker, 26.32 g MPC80 was gradually added to 500 g distilled water. After adding all the powder, data from the UFD and FBRM was acquired every 15 s and 10 s, respectively, for 1800 s. Every 300 s, a 15 mL sample was collected for the solubility index. All tests were done in duplicate.

Statistical analysis

Changes in the powder dissolution characteristics observed by the proposed UFD-based method were analyzed by a repeated measures design using the PROC GLM procedure of SAS (Version 9.4, SAS Institute Inc., Cary, NC).

Results and discussion

Optimization of method parameters

From the parameter optimization studies, a 5% (w/w) concentration was found to be the optimal concentration. In order to optimize the powder concentration, ultrasound velocity and attenuation curves were obtained with MPC concentrations 2.5, 5, 7.5, and 10% w/w. There was an increasing observable trend in ultrasound attenuation and velocity plots during dissolution of MPC for concentrations 5, 7.5, and 10% solutions, and were found to be acceptable for further studies (data not shown). However, 2.5% concentration did not provide an acceptable trend for ultrasound velocity and attenuation and was not considered for subsequent experiments. Keeping in view the time required for addition of MPC to water, it was decided that a 5% solution was optimum to acquire ultrasound data using an UFD for characterizing powder dissolution.

For the stirring conditions, the overhead stirrer speed was set at 900 rpm during powder addition to reduce the time required to wet all the powder particles. Subsequently, the stirrer speed was reduced to 400 rpm for the remainder of the experiment. Yu and Erickson (2008) reported that the stirrer speed below 400 rpm was not sufficient to keep the powder particles in suspension. On the other hand, speed above 400 rpm led to formation of air bubbles and consequently a poor ultrasound signal.

During optimization of ultrasound path length (distance between the reflector plate and the transducer), it was observed that the time required for the second echo to reappear was shorter for shorter ultrasound path lengths. It was found from the preliminary experiments that the optimal path length was 18±0.5 mm. As suggested by the UFD manufacturer and data from preliminary experiments, a damp of 50 ohms and energy level of 100 V were selected. The final

method parameters that were utilized in the evaluation of the proposed method are provided in Table 4.1.

Table 4-1 Parameters used in the proposed UFD-based method

Parameter	Selected Level
Powder concentration (%) (w/w)	5
Temperature (°C)	40 ±0.1
Ultrasound path length (mm)	18±0.5
Damp (ohms)	50
Energy (Volts)	100
Stirring speed (rpm)	
i. During powder addition	900
ii. During data collection	400
Data collection	Every 15 seconds for 1800s (after powder addition)

Evaluating the method

In order to evaluate the method, dissolution behavior MPC80 powders stored at 25 °C and 40 °C for up to 4 weeks were utilized. According to Anema et al. (2006), MPC85 stored at 20 °C showed only a little change in solubility over a storage time of 60 days. However, the solubility of MPC85 decreased exponentially with storage temperature and time. Similarly, in the present study, we also expected a reduction in the solubility of MPC80 and be able to capture the change in solubility characteristics using the proposed UFD-based method.

Relative ultrasound velocity

When MPC80 was added to water the ultrasound signal disappeared, and consequently the relative velocity began to fluctuate. Over time, the ultrasound signal gradually reappeared. The time for the signal to reappear increased as the storage time of powder increased, indicating a loss of solubility. The relative ultrasound velocity at 1800 s was found to be 0.99 for fresh powder and 0.98 for powder stored at 25 °C for 4 weeks. Figure 4.3A shows a typical relative

velocity profile obtained for fresh powder. As we can observe from Figure 4.3A, the relative velocity obtained for the fresh powder samples fluctuated approximately for the first 350 s. On the other hand, the relative velocity obtained for the powders stored at 25 °C for 4 weeks fluctuated for 700 s and subsequently attained a stable value (Figure 4.3B). After 3 weeks storage of MPC at 40 °C, the relative ultrasound velocity fluctuated during the entire experimental period of 1800 s (Figure 4.3C).

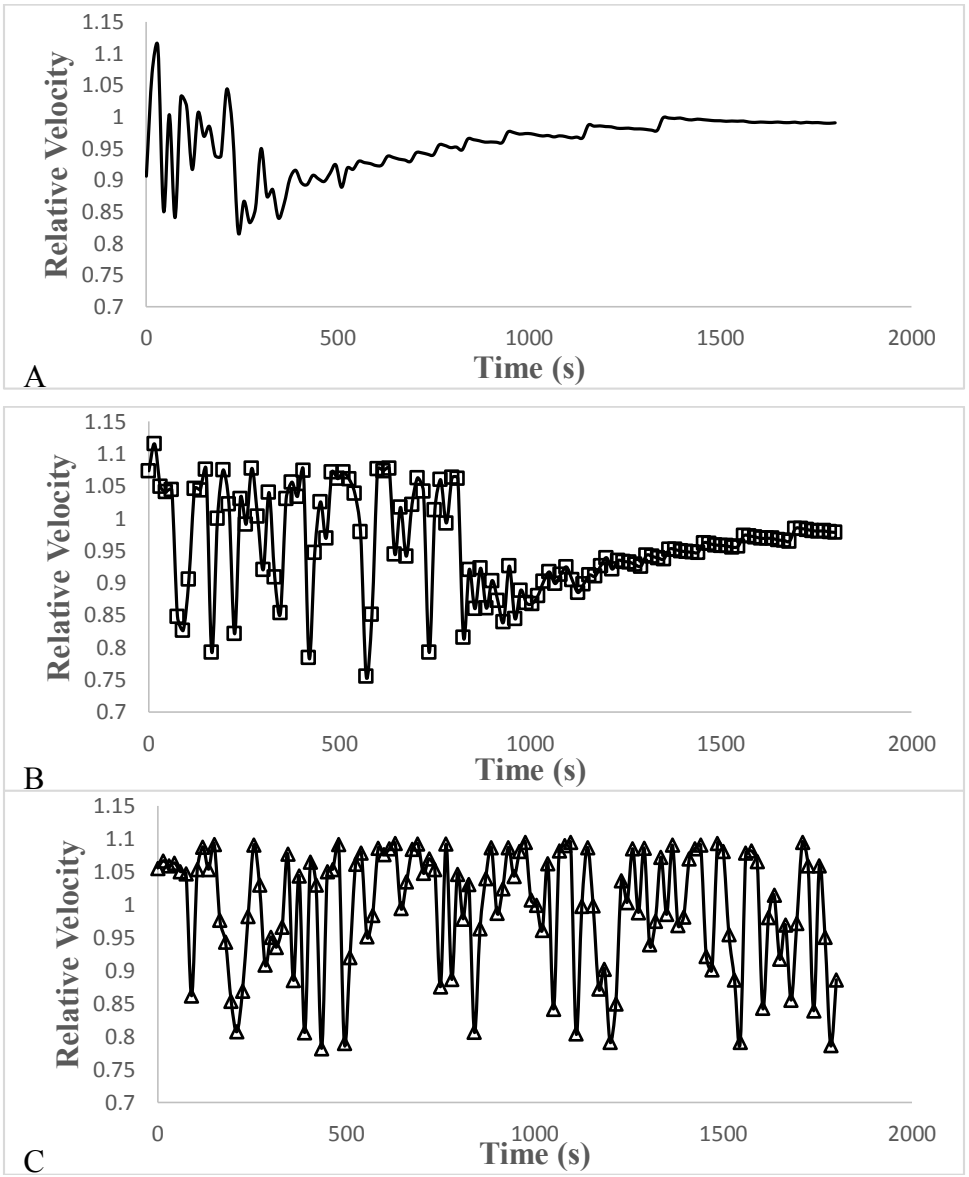

Figure 4-3 Profiles of ultrasound relative velocity obtained from the UFD for fresh powder (A), powders that have been stored at 25°C for 4 weeks (B), and powders that have been stored at 40°C for 4 weeks (C).

Richard et al. (2012) noticed a similar reduction in the ultrasound signal and attributed the reduction in ultrasound signal to water entering into the powder particles and consequently releasing the air from the powder particles into the solution. Yucel and Coupland (2010) found a similar change in ultrasound velocity immediately after the addition of lactose to water and attributed this to the air bubble formation in the system. Interestingly, in the proposed method, the fluctuation in relative ultrasound velocity was found to strongly depend on the storage time and temperature of the powder and can be used as a parameter to characterize powder dissolution behavior.

In order to quantify the changes in the powder dissolution characteristics from the relative ultrasound velocity, the standard deviation of relative ultrasound velocity between 900 and 1800 s was derived as a parameter. Between 900 and 1800 s, fresh powders showed a relatively stable velocity profile. Powders with a longer storage time were still increasing or fluctuating and this led to an increased standard deviation. Figure 4.4 shows the calculated relative velocity standard deviation for the powders stored at 25°C and 40°C.

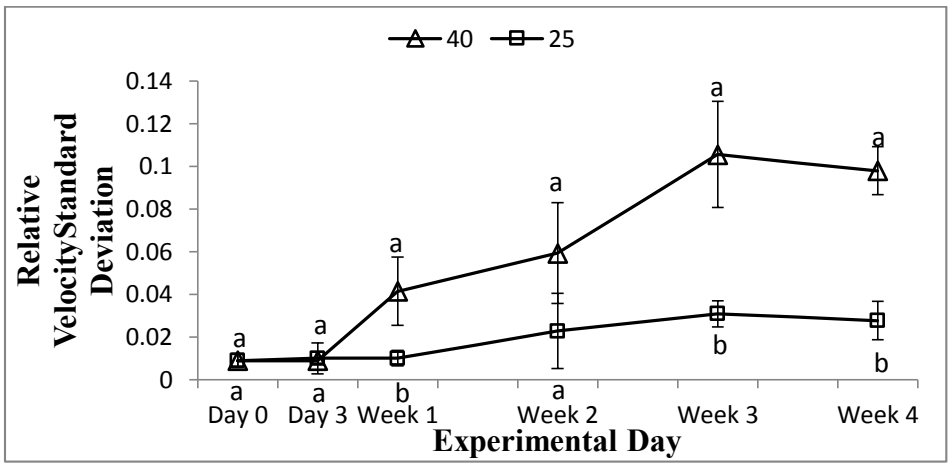

Figure 4-4 Relative ultrasound velocity standard deviation from 900s-1800s extracted from relative velocity data collected with the UFD on each experimental day for powders stored at 40°C and 25°C.

The error bars represent the standard error.
Different lowercase letters differ between storage temperatures ($P < 0.05$).

The relative velocity standard deviations for powders on Day 0, Day 3, and Week 2 were not significantly ($P>0.05$) different for powders stored at 25 °C and 40 °C. This indicates that the powder dissolution characteristics cannot be differentiated using the relative velocity alone as an indicator. However, relative velocity standard deviation was significantly different ($P<0.05$) for the powders stored at 25 °C and 40 °C on experimental Week 1, Week 3, and Week 4. Meyer et al. (2006) observed that the ultrasound velocity measurements were not sufficient to characterize the reconstitution quality of dairy powders.

Ultrasound attenuation

Figure 4.5A shows the changes in ultrasound attenuation during dissolution of powders stored for day 0, Week 1 and Week 4 at 25 °C. In order to simplify the plot, day 3, week 2, and week 3 data were omitted from Figure 4.5A. During dissolution, the ultrasound attenuation for a fresh powder increased during the first 510 s and remained relatively stable for the remainder of the experiment. As the storage time increased, the ultrasound attenuation increased at a slower rate. Stabilizing time for week 1 and week 4 samples stored at 25 °C was found to be around 750 and 950 s, respectively. At the end of the 30 min dissolution time, the ultrasound attenuation was found to be approximately 0.07 Neper/mm for the MPC samples stored at 25 °C. Figure 4.5B shows the changes in ultrasound attenuation during dissolution of powders stored for Day 0, Week 1 and Week 4 at 40 °C. Also at 40 °C, an increase in the ultrasound attenuation was delayed as the powder storage time increased. It is evident from Figures 4.5A and 4.5 that the proposed method was able to differentiate the changes in dissolution characteristics for powders stored at 25 °C and 40 °C, respectively.

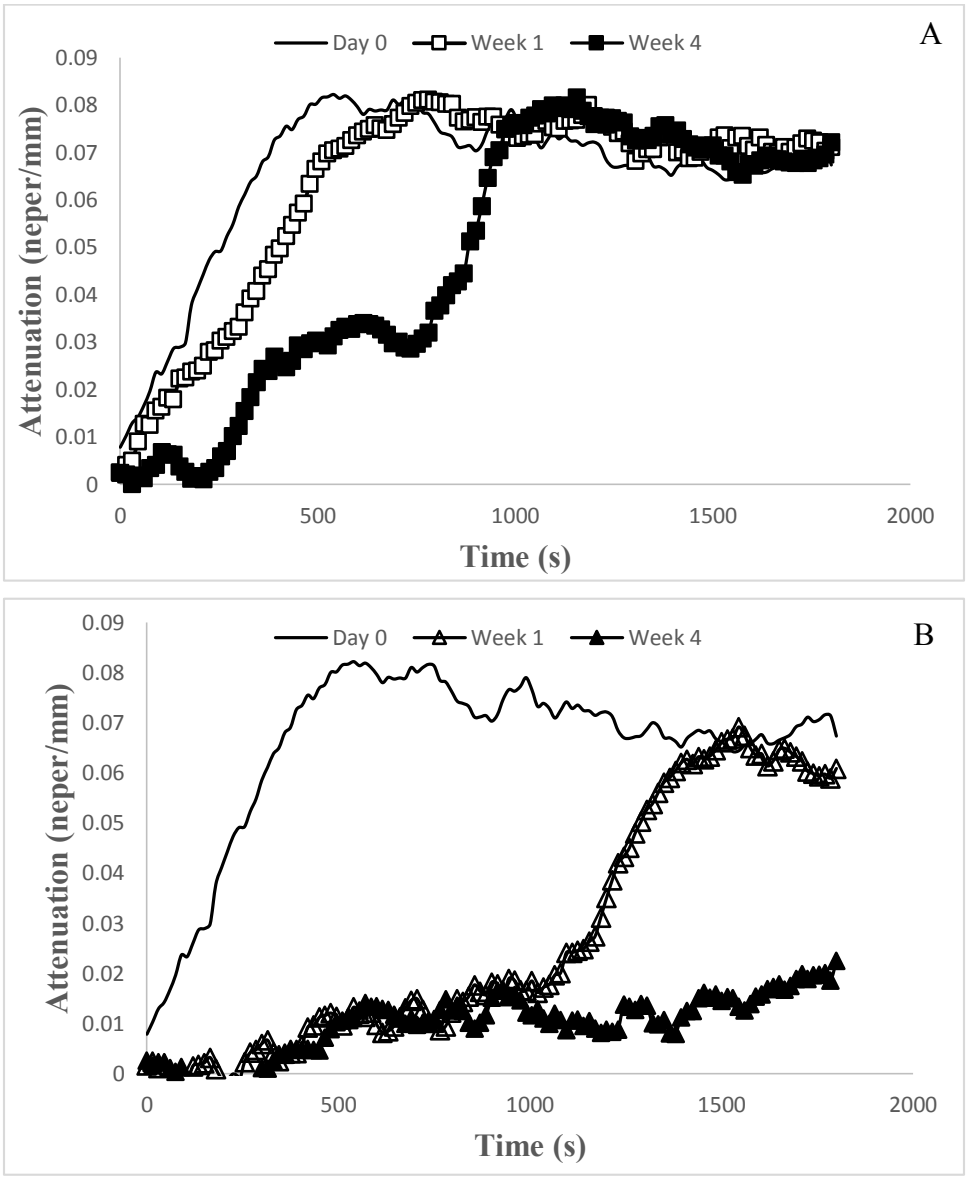

Figure 4-5 Attenuation curves from data collected with the UFD for Day 0, Week 1 and Week 4 for powders stored at 25°C (A) and 40°C (B).

To quantify the changes in the attenuation curve, area under the attenuation curve, peak height, and peak time were derived from the attenuation data (Figures 4.5A and 4.5B). Figure 4.5 show the changes in attenuation parameters as the storage time and temperature increased. Figure 4.6A shows the changes in the area under the curve over the 4 week storage period for the powders stored at 25 °C and 40 °C.

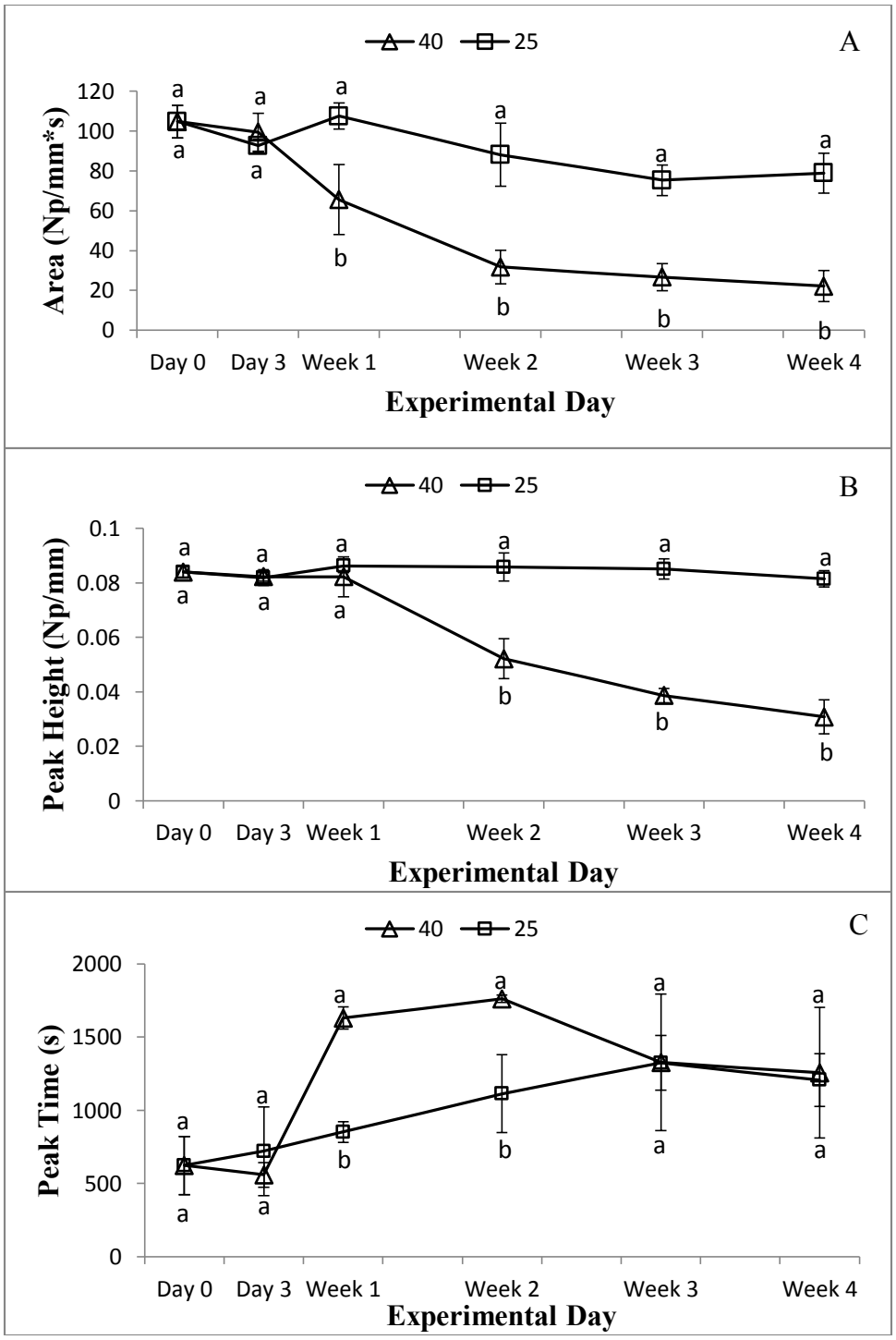

Figure 4-6 Area under the attenuation curve (A), Peak Height (B), and Peak Time (C) extracted from attenuation data collected with the UFD on each experimental day for the powders stored at 25°C and 40°C.

The error bars represent the standard error.
Different lowercase letters differ between storage temperatures ($P < 0.05$).

As the storage time and temperature increased, the area under the curve decreased, indicating loss of solubility. No significant differences ($P>0.05$) were observed on Day 0 and Day 3 between the powders stored at 25 °C and 40 °C as observed by the proposed method. However, the powders stored for more than a week were significantly different ($p<0.05$) at 25 °C and 40 °C. Anema et al. (2006) reported a half-life of 5.7 days for MPC85 stored at 40 °C. For fresh powders, the area was around 100 Np*s/mm. After 4 weeks of storage at 25 °C, the area was reduced by 24%, and powders stored at 40 °C experienced a 78.5% reduction in area under the attenuation curve.

Figures 4.6B and 4.6C show the changes in the attenuation peak height and peak time for the powders stored at 25 °C and 40 °C, respectively, during storage. It was observed that the peak height decreased and peak time increased as the storage time and temperature increased. With the peak height, powders stored at 25 °C and 40 °C were significantly different ($p<0.05$) on Week 2, Week 3, and Week 4. When observing the peak time, a significant difference ($p<0.05$) was only noticed for Week 1 and Week 2. From Figures 4.6A, 4.6B, and 4.6C, it can be observed that the area under the attenuation curve followed by peak height parameters were the most informative features to characterize the powder dissolution behavior. Fresh powders had a peak height of 0.0841 Np/mm with a peak time of 620 s, whereas powders stored for 4 weeks at 25 °C had a peak of height and peak time of 0.075Np/mm and 1205 s, respectively. When the powders were stored at 40 °C for 4 weeks, the peak height was below 0.03 Np/mm and the peak time was around 1250 s.

FBRM

The FBRM tracked the number of fine (<10 μm), medium (10-50 μm), and large (50-150μm) particles as a function of time during dissolution of MPC. Figure 4.7 shows the changes

in fine particle counts obtained during dissolution of fresh MPC, MPC stored at 25 °C for 4 weeks, and MPC stored at 40 °C for 4 weeks.

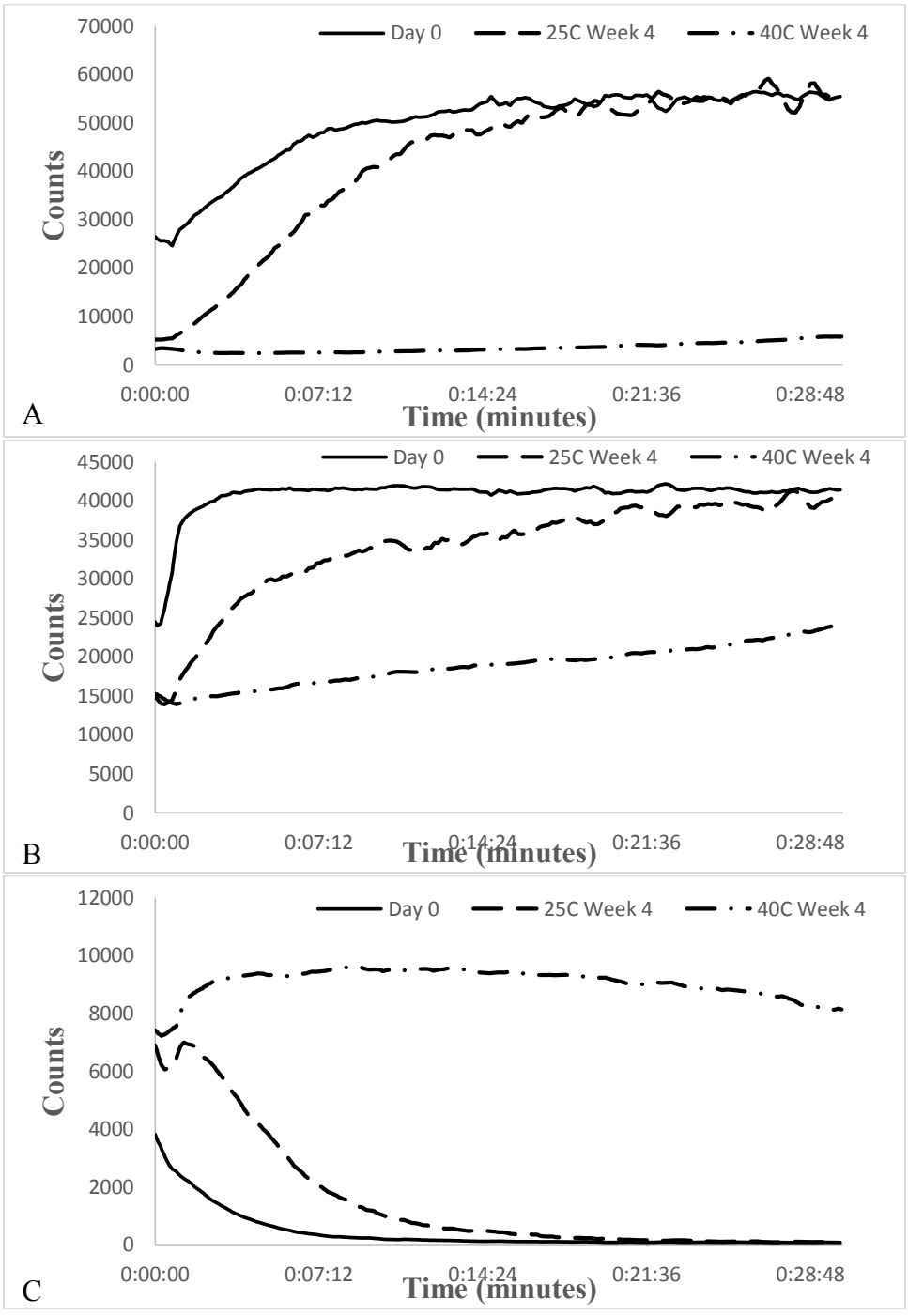

Figure 4-7 Change in fine (A), medium (B), and large (C) counts obtained from the FBRM for Day 0, and powders that have been stored at count 25°C and 40°C for 4 weeks during an experiment.

It is evident from Figure 4.7A that the rate of increase in fine counts reduced as the storage temperature increased. In a study using the FBRM, Fang et al. (2011) noticed that the dissolution rate decreased as the storage temperature and time increased for MPC powders. Fang et al. (2006) also described the initial dissolution rate as the slope of the chord length plot over time, and indicated that the greater magnitude of slope implies a faster dissolution rate of powder. In the current study, fresh powders reached an equilibrium state at a faster rate than the stored powders. Similarly, medium particle counts also increased during the dissolution of MPC (Figure 4.7B). On the other hand, the large particle counts decreased and reached a minimum depending on the MPC quality (Figure 4.7C). The large aggregates of MPC powder disintegrated into medium and fine particles and consequently caused an increase in the counts for fine and medium particles. Over the course of the dissolution, the fine and medium particles reached a maximum that was maintained for the remainder of the experiment. Overall, the FBRM captured the changes between fresh powders and powders that had been stored for 4 weeks at 25 °C and 40 °C.

Solubility

Over the 4-week storage period, the powders stored at 25 °C did not experience a major change in solubility as measured using the solubility index. Anema et al. (2006) also reported that the MPC85 stored at 20 °C showed only a little change in solubility over 60 day storage. However, the solubility was reduced to 47.7% for the powders stored at 40 °C for 4 weeks. Anema et al. (2006) reported that the solubility of MPC85 stored at 40 °C was acceptable only for the first 2 days and decreased rapidly over the next 10 days. In the present study, MPC80 solubility at 40 °C was approximately 97% on Week 1 and reduced rapidly thereafter. Figure 4.8 presents the solubility on each experimental day for the MPC powders stored at 25 °C and 40 °C.

A significant difference ($p<0.05$) was not observed between the 25 °C and 40 °C until Week 2. This indicates that the solubility index as a method was less sensitive in capturing the changes in powder dissolution characteristics.

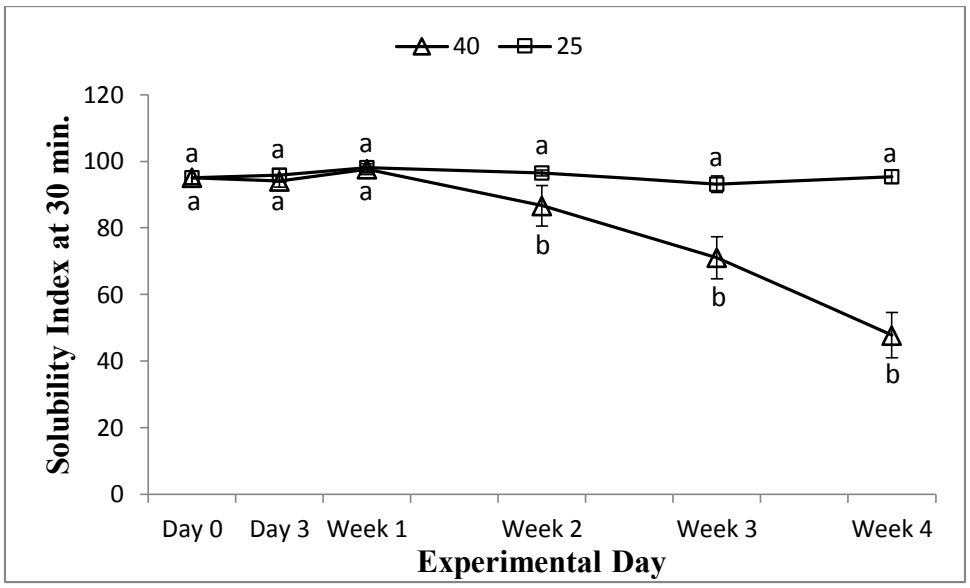

Figure 4-8 Solubility Index at 30 minutes on each experimental day for powders stored at 25°C and 40°C.
The error bars represent the standard error.
Different lowercase letters differ between storage temperatures ($P < 0.05$).

Comparing ultrasound, FBRM, and solubility data

For powders to dissolve quickly, water must be able to penetrate the particles (Richard et al., 2012). However, MPC powders that have been exposed to high temperatures for long periods of time produce a shell structure that inhibits water from penetrating the particle and reduces the dissolution rate (Fang et al., 2011). The reduction in dissolution rate caused by storage temperature and time was captured by the UFD-based method, as well as solubility index methods. However, the proposed UFD-based method was able to differentiate the powders stored at 25 °C and 40 °C for 1 week. This indicates that the proposed UFD-based method is more sensitive than the solubility method in detecting changes in powder dissolution. As the

dissolution rate decreases, the powders take longer to reach an asymptotic value for the ultrasonic amplitude (Richard et al., 2012). With the powders in this study, the peak time increased as the solubility of the powders decreased. FBRM and solubility index showed that storing the MPC for 4 weeks at 25 °C and 40 °C decreased the dissolution rate and solubility of the powder. The ultrasound data also showed that as the dissolution rate and solubility decreased, the area under the attenuation curve and attenuation peak height decreased, and the attenuation peak time and relative velocity standard deviation increased. Thus, a soluble powder will have a low relative standard deviation, low attenuation peak time, high area under the attenuation curve, and high attenuation peak height.

Conclusions

A new and rapid method using an UFD was developed to characterize the dissolution of high-protein dairy powders, specifically MPC, for this study. FBRM and solubility index were used as reference methods. From the velocity and attenuation graphs, the velocity standard deviation from 900-1800 s, area under the attenuation curve, attenuation peak height, and attenuation peak time were derived to characterize the dissolution of the MPC. The FBRM and solubility index showed that the dissolution rate decreased as the storage time and temperature increased. The derived parameters from the relative velocity and attenuation curves clearly show potential to characterize the powder dissolution. A decrease in solubility caused an increase in the standard deviation of relative velocity and attenuation peak time, and a decrease in the peak height and area under the curve. When used as a routine method to assess the solubility of a powder, the best ultrasound parameters to evaluate are the relative velocity standard deviation from 900s-1800s and area under the attenuation curve. Overall, an UFD can be used on a routine

basis as a low-cost method to characterize the dissolution behavior of high-protein dairy powders.

References

Agarwal, S., R. L. W. Beausire, S. Patel and H. Patel. 2015. Innovative uses of milk protein concentrates in product development. J. Food Sci. 80:A23-A29.

Anema, S. G., D. N. Pinder, R. J. Hunter and Y. Hemar. 2006. Effects of storage temperature on the solubility of milk protein concentrate (MPC85). Food Hydrocoll. 20:386-393.

Chandan, R. C. and A. Kilara. 2011. Dairy Ingredients for Food Processing. Amex, Iowa: Wiley- Blackwell, Amex, Iowa.

Corredig, M., 2009. Dairy-Derived Ingredients Food and Nutraceutical Uses. Boca Raton: CRC Press ; Cambridge : Woodhead Pub, Boca Raton : Cambridge.

Corredig, M., M. Alexander and D. G. Dalgleish. 2004. The application of ultrasonic spectroscopy to the study of the gelation of milk components. Food Res. Int. 37:557-565.

Dolatowski, Z. J., J. Stadnik and D. Stasiak. 2007. Applications of ultrasound in food technology. Acta Sci.Pol., Technol.Aliment. 6:89-99.

Dukhin, A. S., P. J. Goetz and B. Travers. 2005. Use of ultrasound for characterizing dairy products. J. Dairy Sci. 88:1320-1334.

Fang, Y., C. Selomulya and X. Chen. 2008. On measurement of food powder reconstitution properties. Drying Technol.26:3-14.

Gunasekaran, S and C. Ay. 1996. Milk coagulation cut-time determination using ultrasonics. J. Food Process Eng. 19:63-73.

Kneifel, W., P. Paquin, T. Abert and J. P. Richard. 1991. Water-holding capacity of proteins with special regard to milk proteins and methodological Aspects—A review. J. Dairy Sci. 74:2027-2041.

Leemans, V. and M. Destain. 2009. Ultrasonic internal defect detection in cheese. J. Food Eng. 90:333-340.

McClements, D. J. 1995. Chapter 4 - ultrasonic characterization of foods. Pages 93-116 in Characterization of Food. A. G. Gaonkar ed. Elsevier Science B.V., Amsterdam.

Meyer, S., V. S. Rajendram and M. J. W. Povey. 2006. Characterization of reconstituted milk powder by ultrasound spectroscopy. J. Food Qual. 29:405-418.

Mohammadi, V., M. Ghasemi-Varnamkhasti, R. Ebrahimi and M. Abbasvali. 2014. Ultrasonic techniques for the milk production industry. Measurement. 58:93-102.

Nassar, G., F. Lefbvre, A. Skaf, J. Carlier, B. Nongaillard and Y. Noêl. 2010. Ultrasonic and acoustic investigation of cheese matrix at the beginning and the end of ripening period. J. Food Eng. 96:1-13.

Olympus. 2007. EPOCH LTC Ultrasonic Flaw Detector User's Manual. Version C ed. United States of America.

Pico, Y. 2012. Chapter 5 - low-intensity ultrasounds. Pages 117-144 in Chemical Analysis of Food: Techniques and Applications. Y. Picó ed. Academic Press, Boston.

Povey, M. J. W. and D. J. McClements. 1988. Ultrasonics in food engineering. part I: Introduction and experimental methods. J. Food Eng. 8:217-245.

Quinn, J. and D. Paton. 1979. A practical measurement of water hydration capacity of protein materials [cereal food products]. Cereal Chem.

Richard, B., M. Toubal, J. Le Page, G. Nassar, E. Radziszewski, B. Nongaillard, P. Debreyne, P. Schuck, R. Jeantet and G. Delaplace. 2012. Ultrasound tests in a stirred vessel to evaluate the reconstitution ability of dairy powders. Innovative Food Science & Emerging Technologies. 16:233-242.

Saggin, R. and J. N. Coupland. 2002. Ultrasonic monitoring of powder dissolution. J. Food Sci. 67:1473-1477.

Wallingford, L. and T. P. Labuza. 1983. Evaluation of the water binding properties of food hydrocolloids by Physical/Chemical methods and in a low fat meat emulsion. J. Food Sci. 48:1-5.

Yu, W. and K. Erickson. 2008. Chord length characterization using focused beam reflectance measurement probe - methodologies and pitfalls. Powder Technol. 185:24-30.

Yucel, U. and J. N. Coupland. 2011. Ultrasonic characterization of lactose crystallization in gelatin gels. J. Food Sci. 76:E48-E54.

Chapter 5 - Effect of protein content and dissolution temperature on the solubility of high-protein dairy powders[2]

Abstract

Processing, storage, dissolution conditions, and the composition of a powder affect the solubility of high protein dairy powders. For example, high inlet and outlet drying temperatures reduce the solubility of high-protein dairy powders. Increasing the storage temperature and time decrease the solubility of milk protein concentrates (MPC) and milk protein isolates (MPI). MPC and MPI are popular ingredients in high-protein food products and have a variety of protein contents. However, few studies have focused on how the protein content affects the solubility of the powder. In addition, the dissolution temperature has been shown to affect the solubility of the powders. This study focused on determining how protein content and dissolution temperature affect the solubility of MPC and MPI. For this study, 11 powders were obtained from a commercial manufacturer. The powders were classified as A, B, C, and D, and they had a protein content of 85%, 87%, 88%, and 90%, respectively. A 5% (w/w) concentration of powder was dissolved in water at 40 °C and 48 °C. The solubility of the MPC and MPI samples were characterized using an ultrasonic flaw detector and focused beam reflectance measurement (FBRM). Ultrasound and FBRM data were collected every 15 and 10 s, respectively, for 1800 s. At both dissolution temperatures, the ultrasound and FBRM data showed that the solubility decreased as the protein content increased. Powders A and B were considered more soluble because they had a lower relative velocity standard deviation, high area under the attenuation curve, high peak height, and low peak time. With the FBRM, the fine and medium particle count

[2] Submitted to Journal of Dairy Science

decreased and large particle count increased as the protein content increased. Increasing the dissolution temperature led to a faster dissolution time. Powders dissolved at 48 °C typically had a lower relative velocity standard deviation, higher area under the attenuation curve, higher peak height, and lower peak time than the powders dissolved at 40 °C. The FBRM showed that powders dissolved at 48 °C reached a stable count before the powders dissolved at 40 °C. Overall, the study showed that increasing the protein content led to a reduction in solubility and increasing the dissolution temperature improved the solubility of the powders.

Introduction

High-protein dairy powders such as milk protein concentrates (MPC) and milk protein isolates (MPI) are added to a variety of dairy and food products to improve the nutritional, sensory, and functional properties. The protein content of MPC and MPI ranges from 40-90%. Generally, powders with a protein content of 80% or above are added to high-protein nutrition bars, meal replacement beverages, and medical nutrition products (Agarwal et al., 2015). MPC and MPI should be soluble to give the products the desired characteristics, but various factors such as processing conditions, composition of the powder, storage conditions, and dissolution conditions affect the solubility.

Lactose, minerals, and water are removed from skim milk during ultrafiltration and diafiltration to concentrate the proteins in their native form (Chandan and Kilara, 2011). However, subsequent processing steps such as evaporation and spray drying partially denature the protein, which leads to a reduction in solubility of the finished product (Augustin et al., 2012; Fang et al., 2012). Various techniques have been proposed to improve the solubility of high-protein dairy powders. The addition of a sodium solution to the retentate before spray drying has been shown to improve the solubility (Schuck et al., 2007). In a study conducted by Augustin et

al. (2012), the addition of a high shear treatment such as homogenization, microfiltration, and ultrasonication improved the solubility of the powder even after 6 months of storage.

The major and minor components of MPC and MPI such as protein, lactose, and minerals influence the solubility. A reduction in rehydration time was observed for powders with a higher lactose and whey protein concentration (Gaini et al., 2006; Gaini et al., 2007). MPC powders have the best solubility immediately after production and the solubility decreases as the storage time and temperature increases. (Anema et al., 2006; Fang et al., 2011; Gazi and Huppertz, 2015).

Studies have shown that increasing the stirring speed and temperature decreased the rehydration time. Jeantet et al. (2010) concluded that increasing the dissolution temperature from 26 °C to 30 °C was more effective than increasing the stirring speed in increasing the solubility of micellar casein powder. Fang et al. (2011) noticed that a higher dissolution temperature improved the ability to detect solubility differences between fresh and aged powders. However, a dissolution temperature at or above 60 °C led to a reduction in solubility due to protein denaturation and aggregation (Fang et al., 2010).

Studies have typically focused on how the processing and storage conditions affect the dissolution of high-protein dairy powders. Limited research has been conducted on quantitatively determining the effect of protein content and dissolution temperature on the solubility of high-protein dairy powders. For this study, the objective was to determine the effect of protein content and dissolution temperature on the solubility of MPC and MPI as measured by an ultrasonic flaw detector and FBRM.

Materials and methods

Experimental design

From a commercial manufacturer within the United States, 11 powder samples were obtained and the dissolution characteristics of powders were evaluated at 40 °C and 48 °C using the UFD-based method and focused beam reflectance measurement (FBRM). After examining the composition of all the powders, as provided by the manufacturer, we divided the powders into four categories based on their protein content. Powders A, B, C, and D had a protein content of 85%, 87%, 88%, and 90%, respectively. Powders A and B both contained three lots and powders C and D contained four lots and one lot, respectively.

Experimental setup

Figure 4.1. shows the experimental setup consisting of an UFD (Epoch LTC, Olympus Scientific Solutions, Waltham, MA), FBRM (Particle Track E25, Mettler Toldeo, Columbus, OH), an immersion transducer (V303-SU; Olympus Scientific Solutions, Waltham, MA) in a holder, and a four-bladed overhead stirrer (Caframo, Georgian Bluffs, Ontario, Canada) that was placed 10mm from the bottom of the beaker. A temperature-controlled water bath (Fisher Scientific, Pittsburgh, PA) was used to maintain the powder dissolution temperature at 40 °C and 48 °C.

Ultrasonic flaw detector (UFD)

An UFD in pulse-echo mode was connected to a 1 MHz immersion transducer. The ultrasound pathlength was kept constant at 18±0.5 mm with a stainless steel holder. A detailed description about the construction of the holder is located in Hauser and Amamcharla (2016). The transducer was adjusted until two distinct peaks appeared. The water was allowed to reach

the dissolution temperature. The stirrer was set 400 rpm and ultrasound data was collected for water at the dissolution temperature. Then the powder was added with the stirrer set at 900 rpm.

Deriving parameters from UFD

The method for exporting the ultrasound data and calculating the velocity, relative velocity, and attenuation can be found in Hauser and Amamcharla (2016). Ultrasound relative velocity and attenuation were plotted against powder dissolution time. From these curves, the standard deviation of relative ultrasound velocity from 900 -1800 s, attenuation peak height (maximum attenuation), attenuation peak time (time to reach maximum attenuation), and area under the attenuation curve were extracted to characterize powder dissolution. The area under the attenuation curve was calculated using the trapezoidal rule. The derived ultrasound parameters were compared to the powders' protein content to understand how protein content influenced the powders' solubility.

FBRM

A FBRM was also used to monitor and evaluate the dissolution behavior of the powders. The FBRM was set at a 30° angle and set 20 mm from the bottom of the beaker. Data from the FBRM was acquired with the icFBRM 4.3 (Mettler Toledo, Columbus, OH) program. The program categorized the particles based on their chord lengths. Counts were obtained for particles in the following categories: fine (<10 μm), medium (10-50 μm), and large (50-150 μm) particles. The change in counts allowed the dissolution to be characterized. This study focused on particles that were up to150 μm. The FBRM has a weighting function that can be applied to the counts and chord length distribution. The unweighted distribution is sensitive to changes for the smaller particles and a square weight is sensitive to large particles (Huang et al., 2009) For

this experiment, an unweight distribution was used. To determine the solubility, the change in counts over time and the counts at 0 s, 300 s, 900 s, 1200 s, 1500 s, and 1800 s were examined

A similar method as Fang et al. (2010) was used to determine the mean particle size for particles in the solution. A 5% (w/w) concentration of aged MPC80 with known dissolution characteristics was dissolved for 30 minutes at 48 °C. The solution was centrifuged at 700 x g for 10 minutes and the particle size distribution was obtained for the supernatant and the sediment.

Evaluating the powders

To evaluate the powders, 11 powders were obtained from a commercial manufacturer and classified as powder A, B, C, or D. Each powder was characterized using the UFD and FBRM. Before adding the transducer to the sample, the distance was collected with the UFD by placing the transducer in room temperature water. For all the samples, a 5% (w/w) concentration was used. In a 1 L beaker, distilled water was allowed to reach the dissolution temperature and the stirrer was set at 400 rpm. Then the stirrer was set to 900rpm and the powder was added to the water within 3 minutes. After adding all the powder, the stirrer was set to 400 rpm and data from the UFD and FBRM was acquired every 15 s and 10 s, respectively, for 1800 s. All tests were done in duplicate. From the ultrasound data, four parameters were extracted from the ultrasound relative velocity and ultrasound attenuation curves.

Statistical analysis

Changes in the powder dissolution characteristics observed by the UFD-based method and FBRM methods were analyzed using the PROC GLMMIX procedure of SAS (Version 9.4, SAS Institute Inc., Cary, NC). The ultrasound parameters were compared for the protein content and at the different dissolution temperatures.

Results and Discussion

MPC and MPI do not have a standard of identity. However, they have GRAS notification (GRAS Notice No. GRN 000504). MPC and MPI are generally described as having casein and whey proteins in the same proportion that is observed in fluid milk. MPCs typically have a protein content between 40% and 85% and MPIs have a protein content above 85% (Agarwal et al., 2015). The name of the powder indicates the protein content of the powder. For example, MPC80 and MPI90 would have a protein content of 80% and 90%, respectively. The powders used in the study had a protein content ranging from 85% to 90%.

The composition for the powders A, B, C, and D is in Table 5-1. The protein content was significantly different ($P<0.05$) for all the powders. To produce a higher protein in MPC and MPI, lactose is removed using ultrafiltration and diafiltration (Agarwal et al., 2015).As can be observed, the lactose content decreased as the protein content increased. The lactose content was not significantly different for powders A and B ($P>0.05$) and for powders C and D ($P>0.05$). For powders A and C as well as powders A and D, the lactose content was significantly different ($P<0.05$). When the protein content increased from 85% to 90%, ash and lactose content decreased by approximately 14% and 60%, respectively.

Table 5-1 Composition of all the powder samples

Powder		Component				
Lot	Type	Protein/TS, %	Moisture, %	Lactose, %	Fat, %	Ash, %
15054	A	85.55	5.13	6.47	1.07	6.60
15047	A	85.60	5.19	5.31	1.18	6.71
15044	A	85.68	5.06	5.02	1.14	6.69
Average A		**85.61[a]**	**5.12**	**5.60[a]**	**1.13[a]**	**6.67[a]**
15056	B	86.78	5.49	4.62	1.18	6.50
15048	B	87.34	5.36	4.34	1.06	6.26
15049	B	87.56	5.12	5.72	1.08	6.47
Average B		**87.23[b]**	**5.32**	**4.89[a]**	**1.11[a]**	**6.41[a]**
14357	C	88.42	4.95	3.20	1.06	5.89
15056	C	88.45	5.04	3.10	1.11	5.84
15048	C	88.45	5.31	3.26	1.02	6.06
15044	C	88.97	5.40	2.22	1.19	5.99
Average C		**88.57[c]**	**5.18**	**2.95[b]**	**1.10[a]**	**5.95[b]**
15020	D	90.02	4.85	2.27	1.18	5.72
Average D		**90.02[d]**	**4.85**	**2.27[b]**	**1.18[a]**	**5.72[b]**

[a-d] mean values within a column with different superscripts differ ($P<0.05$)

Dissolution behavior of MPC and MPI at 40°C

Evaluating the dissolution behavior with an UFD

An ultrasonic flaw detector provides a quantitative and economical alternative to characterize the solubility of high-protein dairy powders (Hauser and Amamcharla, 2016). The UFD collected the time-of-flight and amplitude data to calculate the relative ultrasound velocity and attenuation. From the relative ultrasound velocity and attenuation data, the relative velocity standard deviation from 900-1800 s, area under the attenuation curve, attenuation peak height, and attenuation peak time were calculated. As mentioned by Hauser and Amamcharla (2016), a soluble powder had a low relative velocity standard deviation from 900-1800 s, low peak time, high area under the attenuation curve, and high peak height.

Examining the ultrasound relative velocity

As soon as the powder was added to the water, the ultrasound signal was not detected. Water entering the powder particles released air into the solution and caused a drop in ultrasound signal (Saggin and Coupland, 2002; Richard et al., 2012). The presence of air negatively affects the ultrasound signal by scattering the ultrasound wave (Coupland, 2004). The loss in ultrasound signal led to a fluctuation in relative velocity as the UFD searched for an ultrasound signal. Once a signal was detected, the relative velocity increased and typically reached a final relative velocity of approximately 1.01. To quantify the relative velocity trend, the relative velocity standard deviation between 900 s and 1800 s was extracted from the relative ultrasound velocity.

In a study conducted by Hauser and Amamcharla (2016), fresh MPC80 had a relative ultrasound velocity that fluctuated for a short period of time and had a constant relative ultrasound velocity between 900 s and 1800 s. This resulted in a low relative velocity standard deviation. After the powder had been stored at 40 °C for 4 weeks, the relative velocity fluctuated for the entire experiment, which resulted in a high relative velocity standard deviation. Table 5-2 contains the relative velocity standard deviation for all of the powder samples. The average relative velocity for powders A and B was 0.0071 and 0.0091, respectively, and were determined not to be significantly different ($P>0.05$). Figure 5-1a shows the relative velocity trend for powders A and B and can be used to explain the differences in relative velocity standard deviation.

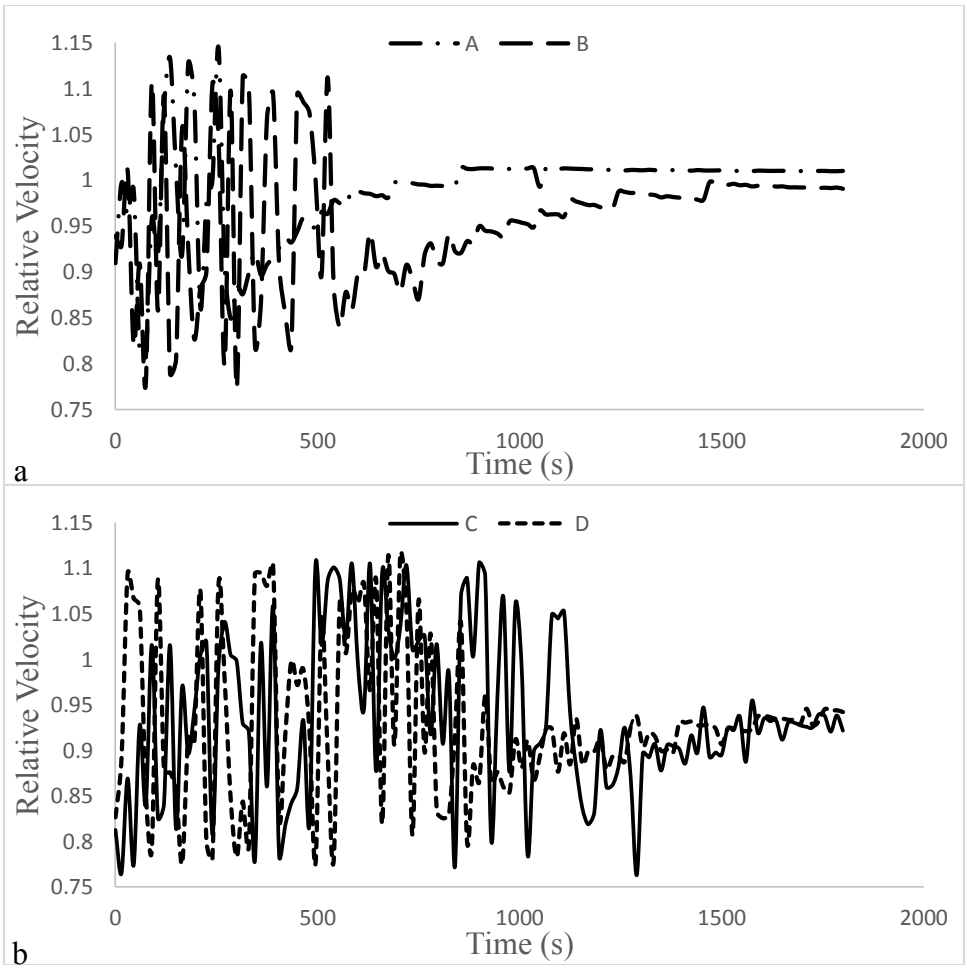

Figure 5-1 Relative velocity trend obtained from data collected with the UFD for powders A and B (a), C and D (b) with a dissolution temperature of 40°C

The lower relative velocity standard deviation for powder A was caused by the powder's ability to reach a relative velocity of approximately 1.01 by 1000 s, whereas powder B was not able to reach a relative velocity of 1.01 until 1500 s.

When the protein content was increased to 88% and 90%, the relative velocity standard deviation increased to 0.0625 and 0.0523, respectively and the relative velocity standard deviation can be found in Table 5-2. The relative velocity standard deviation was not found to be significantly different ($P>0.05$). Figure 5-1b contains the relative velocity trend for powders C and D. As can be observed, the relative velocity for powders C and D fluctuated for a longer

period of time than powders A and B. The relative velocity for powders C and D increased towards the end of the experiment and reached a final relative velocity of approximately 0.095.

As the protein content increased from 85% for powder A to 90% for powder D, the increase in relative velocity standard deviation from powders A to D can be explained by the composition of the powders. Increasing the protein content from 85% to 90% led to a reduction in lactose. Lactose has been shown to decrease the dissolution time since it helps the water enter the core of the powder particle (Richard et al., 2013). With less lactose and more protein in powders C and D, the water penetrated the powder particle and released air into the solution for a longer period of time. Therefore, the ultrasound signal was lost for a longer period of time, which increased the relative velocity standard deviation. Based on the observations from the relative velocity data, we saw that powder A was more soluble than powder B followed by powders C and D. A significant difference was observed ($P<0.05$) between powders A and C, as well as B and C. However, a significant difference was not observed ($P>0.05$) between powders A and D, and powders B and D.

Examining the ultrasound attenuation

Besides the relative velocity, ultrasound attenuation also provided information about the solubility of the powders. Unlike velocity, which was influenced by a solutions concentration, ultrasound attenuation was influenced by particle size distribution. Therefore, attenuation increases as a powder particle disintegrates. To quantify the attenuation curve, the peak height, peak time, and area under the attenuation curve were extracted from the ultrasound attenuation data. Table 5-2 contains the peak height, peak time, and area under the attenuation curve for all the powders.

Figure 5-2 shows the attenuation curve for all the powders.

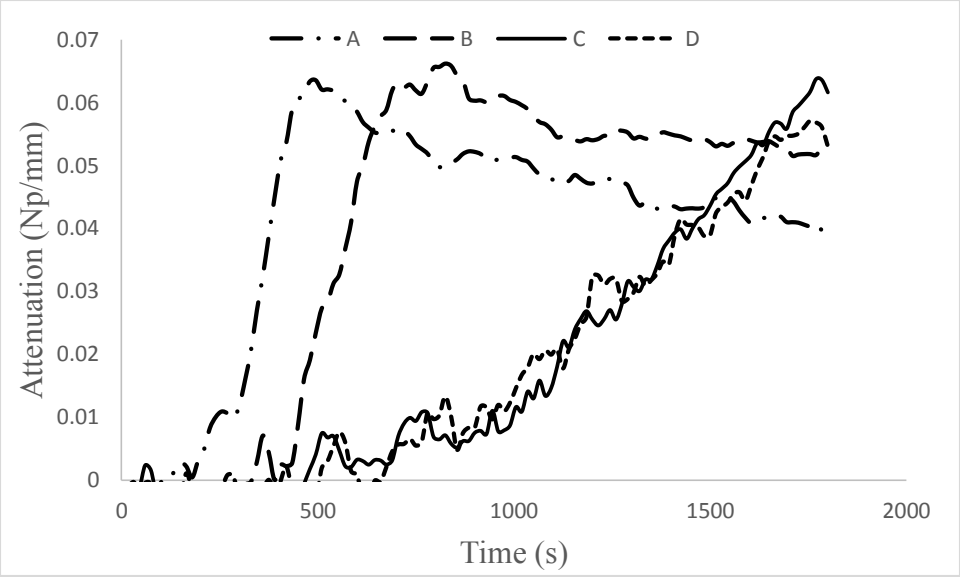

Figure 5-2 Attenuation trend obtained from the data collected with the UFD for powders A, B, C, and D with a dissolution temperature of 40°C

As can be observed, powders A and B had a trend of increasing, reaching a peak and then decreasing. The average peak height for powders A and B was between 0.07 Np/mm and 0.08 Np/mm and the average peak time was between 825 s and 835 s. The peak height and peak time for powders A and B were not significantly different ($P>0.05$). When the protein content increased for powders C and D, the attenuation curve developed a lag time before the attenuation increased. The change in the attenuation curve caused the average peak height for powders C and D to decrease to approximately 0.05 Np/mm and the average peak time increased to 1650 s and 1780 s for powders C and D, respectively. A significant difference was not observed ($P>0.05$) between powders C and D for the peak height and peak time. The reduction in peak height and increase in peak time indicated that the solubility decreased as the protein content increased. With the peak height, a significant difference was not noticed ($P>0.05$) between powders A and C and powders A and D, but a significant difference was observed ($P<0.05$) between powders B

and C. For the peak time, a significant difference was observed ($P<0.05$) between powders A and C as well as D and powders B and C, as well as D.

To better quantify the changes in the attenuation curve, the area under the attenuation curve was calculated. The average area under the attenuation curve for powders A and B was between 66 Np*s/mm and 69 Np*s/mm, respectively. A significant difference ($P<0.05$) was not observed between powders A and B. The area decreased by approximately 70% as the protein content increased from 85% to 90%. For powders C and D, the average area under the attenuation curve was 23 Np*s/mm and 21 Np*s/mm, respectively. After examining all the ultrasound parameters, we observed that powders A and B were more soluble than powders C and D. Significant differences were noticed ($P<0.05$) between powders A and C, as well as powders A and D. Therefore, the UFD showed that an increase in protein content reduced the solubility.

Monitoring the dissolution behavior with a FBRM

As the powders dissolved, the count for large particles decreased as they disintegrated into fine and medium particles. Subsequently, the count for fine and medium particles increased. Figure 5.3 shows how the fine, medium, and large particle counts changed during an experiment.

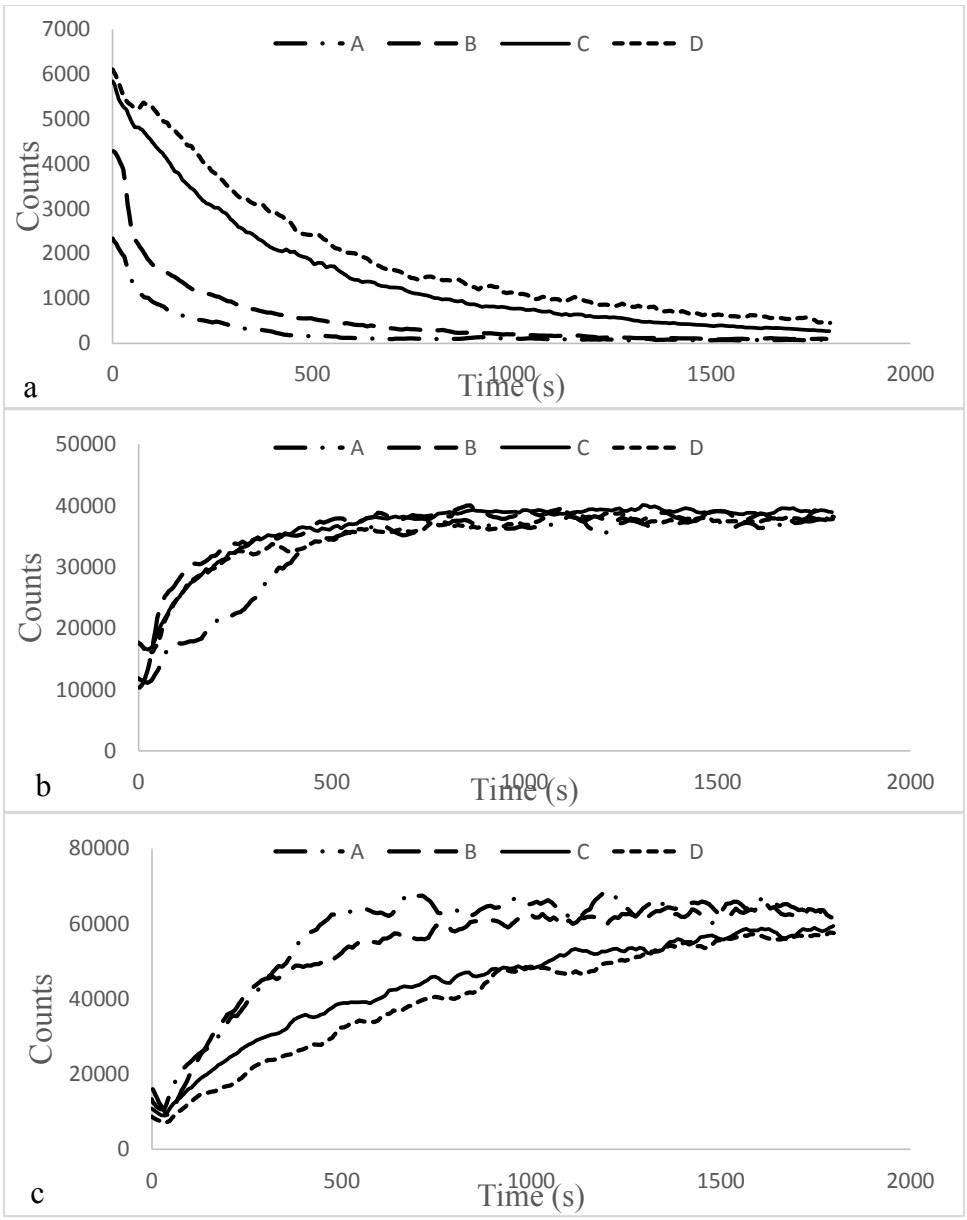

Figure 5-3 Change in large (a), medium (b), and fine (c) counts obtained from data collected with the FBRM for powders A, B, C, and D with a dissolution temperature of 40°C

To determine the solubility with an FBRM, Fang et al., (2011) compared the dissolution rate constant and the final particle size for fresh and aged MPC. Fresh MPC was the most soluble and had a high dissolution rate constant and lower final particle size. A similar method was used to determine the solubility of the powder for this study.

Figure 5-3a shows the change in counts for large particles. As can be observed, the large particle counts for powders A and B decreased rapidly, whereas the large particle counts for powders C and D had a gradual reduction in counts. Throughout the experiment, powder A and B had lower large particle counts than powders C and D. At 0 s, powders A and B had a large particle count around 3,000, whereas powders C and D had a large particle count around 6,400. The difference in large particle counts increased at 300 s. Powders A and B had counts of 490 and 710, respectively, and the large particle counts for powders C and D was 7 times higher with large particle counts of 2,500 and 2,300, respectively. By 1800 s, powders A and B had a large particle count between 70 and 75. Powder A reached the lowest large particle count around 1200s and powder B reached the lowest large particle count around 1500 s. On the other hand, for powders C and D (88% and 90% protein content, respectively), the counts for large particles at 1800s increased were found to be 610 and 450, respectively.

Once the large particles disintegrated into smaller particles during dissolution, the counts for medium and fine particles increased, as seen in Figure 5-3b and Figure 5-3c. With the medium particles, powders A and B had a medium particle count of 12,500 and 12,100, respectively, at 0 s. The medium particle count at 0 s increased as the protein content increased from to 88% and 90%, with powders C and D having a count of 17,000 and 18,000, respectively. By 900 s, all the powders had a medium particle count of approximately 36,000 and maintained the count for the remainder of the experiment. The fine particles had a similar increasing trend for counts. At 0 s, powders A and B had a fine particle count of 12,000 and 13,000, respectively. Powders A and B were able to reach a fine particle count of 62,000 by 900 s and maintained the count for the remainder of the experiment. When the protein content increased from 85% to 88%

and 90%, the fine particle counts gradually increased. For powders C and D, the fine particle counts increased from 8,000 at 0 s to 55,000 at 1800 s.

A decreasing final count for fine and medium particles and an increasing count for large particles indicated a reduction in solubility. Powders A and B had higher counts for fine and medium particles, which indicated they were more soluble than powders C and D, which had a lower count for fine and medium particles. For powders A and B, the ability of powder A to reach the maximum count for fine particles sooner indicated that powder A was more soluble than powder B. Overall, the FBRM showed that an increase in protein content negatively affected the solubility.

The UFD and FBRM results match those of Crowley et al. (2015). MPC powders with increasing protein content were examined for solubility. To determine the solubility, a specific centrifuging procedure was used and the sediment was related to the solubility. Powders with a higher protein content had a higher sediment height, which indicated that the powder was less soluble. We found that a reduction in relative velocity standard deviation, increased area under the attenuation, reduction in fine and medium particle counts at 1800 s, and an increase in large particle counts at 1800 s indicated the powders with a lower protein content were more soluble.

Dissolution behavior of MPC and MPI at 48°C

To decrease the dissolution time, a higher dissolution temperature can be used. In this study, we raised the dissolution temperature from 40 °C to 48 °C. Fang et al. (2010) found that 50 °C was generally the best dissolution temperature. If the temperature exceeded 50 °C, the proteins denatured and aggregated. However, a dissolution temperature of 50 °C could not be used because the high temperature would damage the transducer.

Evaluating the dissolution behavior with an UFD

The powders dissolved at 48 °C had the same relative velocity trend as the powders dissolved at 40 °C. Using the same analytical techniques, we observed that the solubility decreased as the protein content increased from 85% (powder A) to 90% (powder D). Increasing the dissolution temperature led to a reduction in relative velocity standard deviation. A significant difference ($P<0.05$) for the relative velocity standard deviation at 40 °C and 48 °C was only observed for powders C and D. Table 5-2 contains the relative velocity standard deviation for all the powders when they were dissolved at 48°C. Figure 5-4a has the relative ultrasound velocity trend for powders A and B.

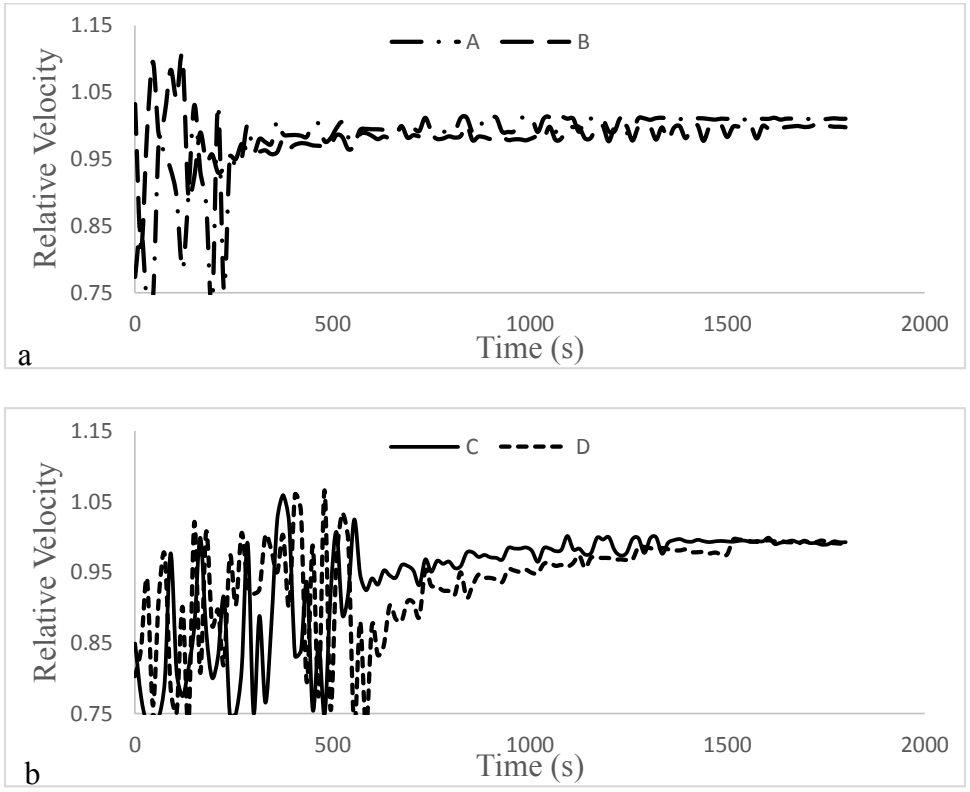

Figure 5-4 Relative velocity trend obtained from data collected from the UFD for powders A and B (a) and powders C and D (b) with a dissolution temperature of 48°C

As can be observed, the relative ultrasound velocity has some dips in relative velocity after a relative velocity of 1.01 was reached. The relative velocity standard deviation for powder B decreased since a relative velocity of 1 was reached at 750 s, instead of 1500 s that was observed when the powder B was dissolved at 40°C. As the temperature of the water increased, the surface tension of the water decreased. When dissolving a powder, the wettability is the powder particle overcoming the surface tension of water. With a lower surface tension, the water entered the powder particle faster, which led to more air being released into the system. This in turn led to a shorter fluctuation time.

A similar change in relative ultrasound velocity led to a reduction in the relative ultrasound velocity trend for powders C and D when they were dissolved at 48 °C. Figure 5-4b contains the relative ultrasound velocity trend for powders C and D. When powders C and D were dissolved at 48 °C, the fluctuation time decreased to 500 s and the relative velocity was able to reach a constant value of 1. The ability of the powder to reach a constant value led to a reduction in the relative velocity standard deviation. The standard deviation decreased more for powders C and D. Powder B experienced a 25% reduction in the relative velocity standard deviation, whereas powders C and D decreased by 63% and 65%, respectively.

Figure 5-5 shows the attenuation curve for all the powders when they were dissolved at 48°C. All the powders had a trend of an increasing attenuation, reaching a peak, and then decreasing. Powders C and D had a lag time before the attenuation increased.

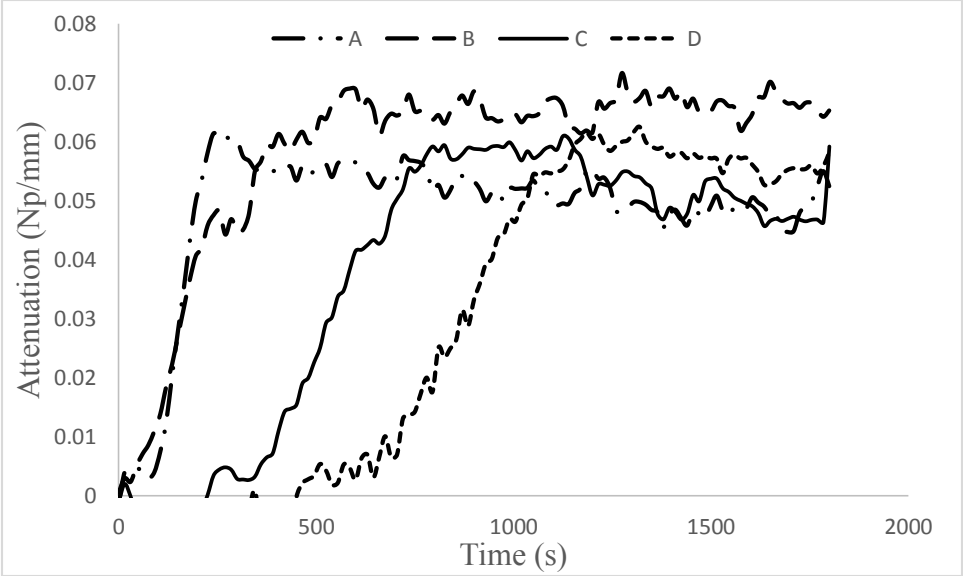

Figure 5-5 Attenuation curve obtained from data collected with the UFD for powders A, B, C, and D with a dissolution temperature of 48°C

Table 5-2 contains the extracted ultrasound attenuation parameters. The peak height increased for all the powders when the dissolution temperature increased to 48 °C. Powders A, B, C, and D had an average peak height of 0.07, 0.078, 0.068, and 0.069 Np/mm, respectively. However, the peak time increased for powders A and B and decreased for powders C and D. When examining the area under the attenuation curve, the area increased by 27%, 27%, 125%, and 145%, respectively, for powders A, B,C, and D. The increased area can be attributed to a faster dissolution rate due to the higher dissolution temperature. A significant difference was observed ($P<0.05$) between the 40 °C and 48 °C dissolution temperature for all the powders. Overall, we observed that the solubility improved with the increased dissolution temperature since a reduction in relative velocity standard deviation and increase in area under the attenuation curve was observed.

Monitoring the dissolution behavior with a FBRM

FBRM data was also collected when the powders were dissolved at 48 °C. The trends for the large, medium, and fine particles was the same as the trends observed when the powder was

dissolved at 40 °C. Using the same analysis technique, the FBRM data showed that powders A and B were more soluble than powders C and D. To determine how the dissolution temperature affected the solubility of the powders, the mean particle size was examined, as well as the time needed to reach the minimum particle size. As can be observed in Figure 5-6a and Figure 5-6b powders A and B were able to quickly reach the minimum mean particle size when the powders were dissolved at 48 °C instead of 40 °C. In Figure 5-6c, it can be observed that the mean particle size of powder C decreased at a slower rate as compared to powders A and B, which had a quicker reduction in mean particle size. For powder C, the dissolution temperature of 48 ° C was able to reach the minimum particle size before the dissolution temperature of 40 °C. Figure 5-6d contains the change in mean particle size for powder D. A dissolution temperature of 48 °C had a similar trend as the 40 °C dissolution temperature. When dissolved at 48 °C, the minimum particle size was reached around 1200 s and when dissolved at 40 °C, the minimum particle size was reached around 1490 s.

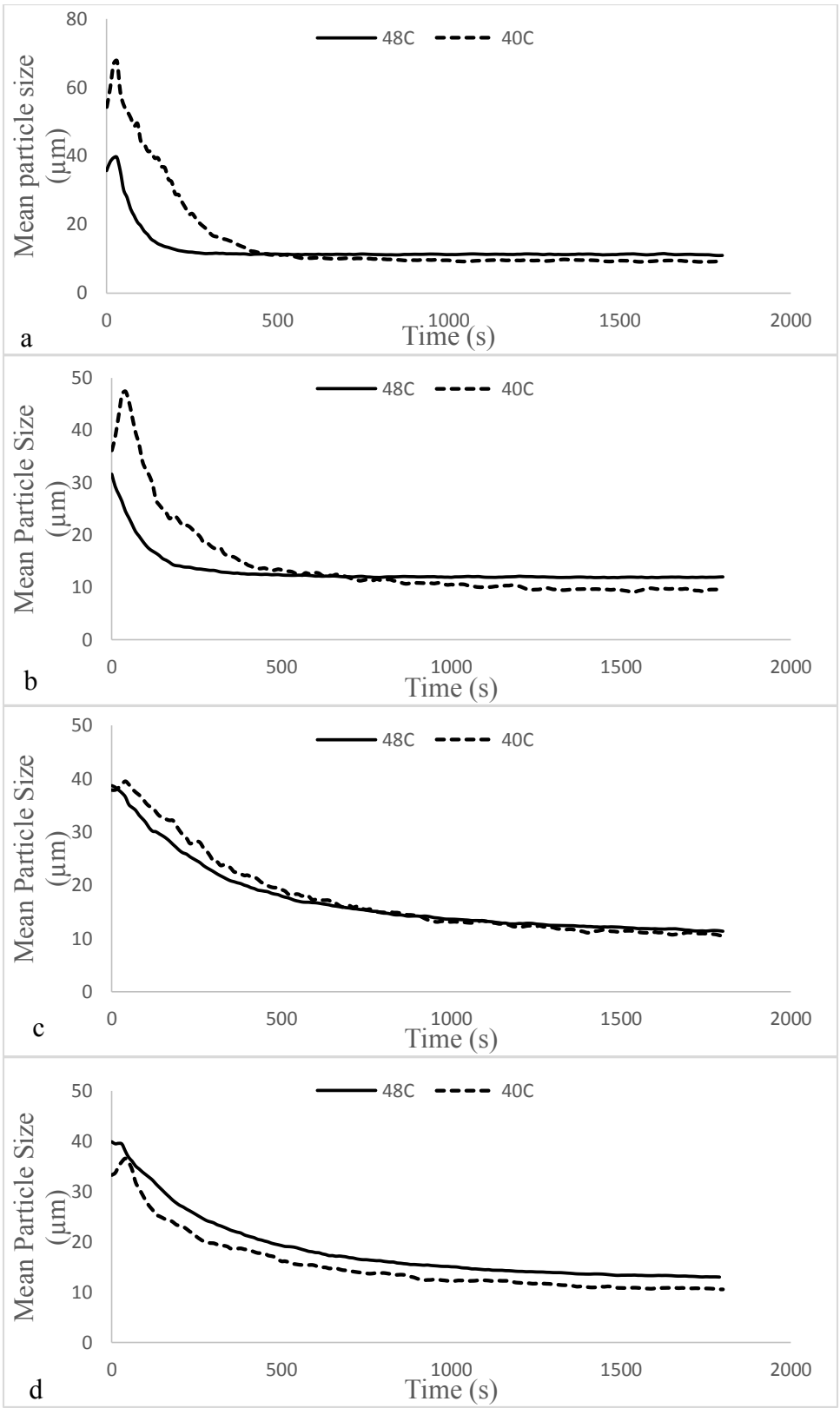

Figure 5-6 Change in mean particle size (µm) obtained from the FBRM for powders A(a), B(b), C(c), and (d) with a dissolution temperature of 40°C and 48°C

As can be observed in all the figures (Figures 5-6 a-d), the powders dissolved at 40 °C had a lower mean particle size. For both dissolution temperatures, the particles were in solution. Fang et al., (2010) stated that a particle is in solution when the particle size was <100 µm. To determine the size, powder was dissolved and then centrifuged. Afterwards, the particle size distribution for the sediment and supernatant were obtained. The supernatant contained the particles that were in solution. We conducted additional research to determine the size of particles in solution. Figure 5-7 contains the particle size distribution for the sediment and supernatant of an aged MPC80 with known dissolution characteristics.

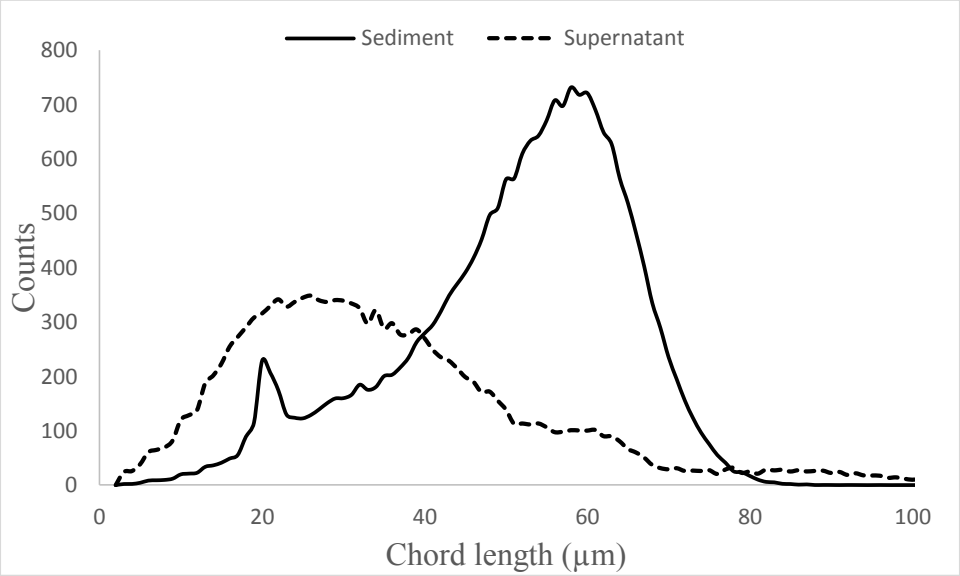

Figure 5-7 Particle size distribution obtained from the FBRM for aged MPC80 supernatant and sediment when dissolved at 48°C

The mean particle size was determined to be 31 µm and 49 µm for the supernatant and sediment, respectively. After examining the particle size distribution, it was hypothesized that particles <50µm were in the solution. Therefore, the particles were in solution at 40 °C and 48 °C. Future research should be conducted to determine if the particle size in solution is lower than 50 µm and the optimal centrifuge conditions to be used to determine the particle size distribution for the supernatant and sediment.

Overall, the FBRM data showed powders with a lower protein content such as powder A were more soluble than powders with a higher content such as powder D, and that an increasing the dissolution temperature from 40 °C to 48 °C improved the solubility of the powders. These results agreed with those of Fang et al. (2010) and Jeantet et al. (2010). The authors found that the dissolution time decreased with an increase in dissolution temperature. Fang et al. (2010) attributed the decreased dissolution time to the powder's ability to readily de-agglomerate. A dissolution temperature of 50 °C typically allowed for the best solubility of MPC and showed more solubility differences for fresh and aged powders (Fang et al., 2010).

Conclusions

The UFD and FBRM data showed that the protein content influenced the solubility of the powder at a dissolution temperature of 40 °C and 48 °C. Increasing the protein content from 85% to 90% led to an increase in relative velocity standard deviation and reduction in area under the attenuation curve, which indicated a reduction in solubility. From the FBRM, a reduction in fine and medium particles and an increase in large particles indicated that the solubility decreased as the protein increased from 85% to 90%. Both the UFD and FBRM showed that the solubility improved when the dissolution temperature increased from 40 °C and 48 °C. The relative velocity standard deviation decreased and the area under the attenuation curve increased as the dissolution temperature increased. The FBRM showed that the powders dissolved at 48 °C had a quicker reduction in mean particle size as compared to the powders dissolved at 40 °C, which had a slower change in mean particle size. Overall, we concluded that the increase in protein content and reduction in lactose led to a less soluble powder, and increasing the dissolution temperature improved the solubility of the powders.

Table 5-2 Ultrasound parameter data extracted from data collected with the UFD for all the powder samples that were dissolved at 40°C and 48°C

Powder		Ultrasound Parameter							
		Relative Velocity Standard Deviation from 900-1800s		Area under the attenuation curve (Np*s/mm)		Peak Height (Np/mm)		Peak Time (s)	
Lot	Type	40°C	48°C	40°C	48°C	40°C	48°C	40°C	48°C
15054	A	0.0100	0.0083	68.24	85.15	0.0732	0.0698	1117.5	982.5
15047	A	0.0017	0.0054	63.59	82.05	0.0619	0.0683	480.0	652.5
15044	A	0.0097	0.0090	66.17	84.55	0.0689	0.0727	885.0	1320.0
Average A		**0.0071^{ax}**	**0.0075^{ax}**	**66.00^{ax}**	**83.92^{ay}**	**0.0680^{abx}**	**0.0703^{ay}**	**827.5^{ax}**	**985.0^{ay}**
15056	B	0.0080	0.0075	74.70	81.03	0.0718	0.0757	855.0	1740.0
15048	B	0.0183	0.0068	61.12	79.10	0.0701	0.0772	1087.5	1140.0
15049	B	0.0010	0.0061	71.52	103.81	0.0662	0.0807	555.0	1200.0
Average B		**0.0091^{ax}**	**0.0068^{ax}**	**69.11^{ax}**	**87.98^{ay}**	**0.0694^{bx}**	**0.0779^{by}**	**832.5^{ax}**	**1360.0^{ay}**
14357	C	0.0320	0.0131	39.73	60.18	0.0655	0.0661	1627.5	1020.0
15056	C	0.0728	0.0262	15.80	48.12	0.0458	0.0726	1777.5	1657.5
15048	C	0.0437	0.0155	30.02	48.77	0.0640	0.0656	1792.5	1515.0
15044	C	0.1015	0.0376	5.69	48.80	0.0260	0.0676	1440.0	1425.0
Average C		**0.0625^{bx}**	**0.0231^{ay}**	**22.81^{bx}**	**51.47^{by}**	**0.0503^{ax}**	**0.0680^{ay}**	**1659.4^{bx}**	**1404.4^{ay}**
15020	D	0.0523	0.0179	20.99	51.63	0.0489	0.0688	1777.5	1290.0
Average D		**0.0523^{abx}**	**0.0179^{ay}**	**20.99^{bx}**	**51.63^{by}**	**0.0489^{ax}**	**0.0688^{ay}**	**1777.5^{bx}**	**1290.0^{ay}**

$^{a-b}$ mean values within a column with different superscript differ ($P<0.05$)

$^{x-y}$ mean values for the dissolution temperatures within an ultrasound parameter that have a different letter differ ($P<0.05$)

References

Agarwal, S., R. L. W. Beausire, S. Patel and H. Patel. 2015. Innovative uses of milk protein concentrates in product development. J. Food Sci. 80:A23-A29.

Anema, S. G., D. N. Pinder, R. J. Hunter and Y. Hemar. 2006. Effects of storage temperature on the solubility of milk protein concentrate (MPC85). Food Hydrocoll. 20:386-393.

Augustin, M. A., P. Sanguansri, R. Williams and H. Andrews. 2012. High shear treatment of concentrates and drying conditions influence the solubility of milk protein concentrate powders.79:459-468.

Chandan, R. C. and A. Kilara. 2011. Dairy Ingredients for Food Processing. Amex, Iowa: Wiley- Blackwell, Amex, Iowa.

Crowley, S. V., B. Desautel, I. Gazi, A. L. Kelly, T. Huppertz and J. A. O'mahony. 2015. Rehydration characteristics of milk protein concentrate powders. J. Food Eng. 149:105-113.

Coupland, J. N. 2004. Low intensity ultrasound. Food Res. Int. 37:537-543.

Fang, Y., C. Selomulya, S. Ainsworth, M. Palmer and X. D. Chen. 2011. On quantifying the dissolution behaviour of milk protein concentrate. Food Hydrocoll. 25:503-510.

Fang, Y., C. Selomulya and X. Chen. 2010. Characterization of milk protein concentrate solubility using focused beam reflectance measurement. Dairy Science & Technology; Dairy Sci.Technol. 90:253-270.

Fang, Y., S. Rogers, C. Selomulya and X. Chen. 2012. Functionality of milk protein concentrate: Effect of spray drying temperature. Biochem. Eng. J. 62:101-105.

Gaiani, C., J. J. Ehrhardt, J. Scher, J. Hardy, S. Desobry and S. Banon. 2006. Surface composition of dairy powders observed by X-ray photoelectron spectroscopy and effects on their rehydration properties. Colloids and Surfaces B: Biointerfaces. 49:71-78.

Gaiani, C., P. Schuck, J. Scher, S. Desobry and S. Banon. 2007. Dairy powder rehydration: Influence of protein state, incorporation mode, and agglomeration. J. Dairy Sci. 90:570-581.

Gazi, I. and T. Huppertz. 2015. Influence of protein content and storage conditions on the solubility of caseins and whey proteins in milk protein concentrates. Int. Dairy J. 46:22-30.

Hauser and Amamcharla. 2016. Development of a method to characterize high-protein dairy powders using an ultrasonic flaw detector. J. Dairy Sci. 99:xxx-xxx. In Press.

Huang, J., G. Kaul, J. Utz, P. Hernandez, V. Wong, D. Bradley, A. Nagi and D. O' Grady. 2010. A PAT approach to improve process understanding of high shear wet granulation through in-line particle measurement using FBRM C35. J. Pharm. Sci. 99:3205-3212.

Jeantet, R., P. Schuck, T. Six, C. Andre and G. Delaplace. 2010. The influence of stirring speed, temperature and solid concentration on the rehydration time of micellar casein powder. Dairy Science & Technology; Dairy Sci.Technol. 90:225-236.

Richard, B., J. F. Le Page, P. Schuck, C. Andre, R. Jeantet and G. Delaplace. 2013. Towards a better control of dairy powder rehydration processes. Int. Dairy J. 31:18-28.

Richard, B., M. Toubal, J. Le Page, G. Nassar, E. Radziszewski, B. Nongaillard, P. Debreyne, P. Schuck, R. Jeantet and G. Delaplace. 2012. Ultrasound tests in a stirred vessel to evaluate the reconstitution ability of dairy powders. Innovative Food Science & Emerging Technologies. 16:233-242.

Saggin, R. and J. N. Coupland. 2002. Ultrasonic monitoring of powder dissolution. J. Food Sci. 67:1473-1477.

Schuck, P., S. Mejean, A. Dolivet, C. Gaiani, S. Banon, J. Scher and R. Jeantet. 2007. Water transfer during rehydration of micellar casein powders. Lait; Lait. 87:425-432.

Chapter 6 - Conclusions

High-protein dairy powders are added to a variety of dairy and food products to improve the nutritional, sensory, and functional properties of the product. If the high-protein dairy powder is not soluble, then the product will not have the desired characteristics. However, current methods used for characterizing the solubility of high-protein dairy powders are time-consuming, subjective, require expensive equipment or skilled technicians. A quantitative and economical alternative to characterize the solubility of high-protein dairy powder is of an ultrasonic flaw detector (UFD).

To develop the UFD-based method, the powder concentration, stirring procedure, pathlength, damp, and energy were optimized. Once the method was developed, milk protein concentrate (MPC) with different solubility characteristics were evaluated. The focused beam reflectance measurement (FBRM) and solubility index were used as reference methods and showed the solubility of the MPC decreased as the storage time and temperature increased. A soluble MPC powder had a low relative velocity standard deviation, high area under the attenuation curve, high peak height, and low peak time.

Besides the storage time and temperature, the protein content and dissolution temperature effected the solubility of high-protein dairy powders. Increasing the protein content from 85% to 90% and reducing the lactose content from 5.6% to 2.3% increased the relative velocity standard deviation and reduced the area under the attenuation curve. Therefore, the solubility of the powder decreased as the protein content increased. When the dissolution temperature increased from 40°C to 48°C, the relative velocity standard deviation decreased and the area under the attenuation curve increased, which meant that the solubility of the powder improved.

Future research with the UFD can focus on developing a UFD set-up that automatically adds the powder and collects the data, and another study could focus on shortening the testing time. With the FBRM, a future study can determine the size of particles (no weight) in solution for different powders, and the optimal centrifuge procedure for separating soluble and insoluble powder particles.

Overall, the UFD was able to detect differences in solubility before the commonly used solubility index method. To assess a powder's solubility, the relative velocity standard deviation and area under the attenuation must be examined. A soluble powder will have a low relative velocity standard deviation and high are under the attenuation curve. The UFD can be used to characterize the solubility of high-protein dairy powders.

Appendix A - Collecting and analyzing the ultrasound data

Equipment and materials needed

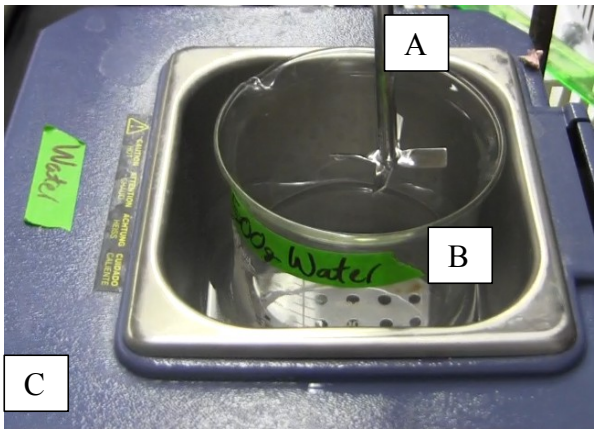

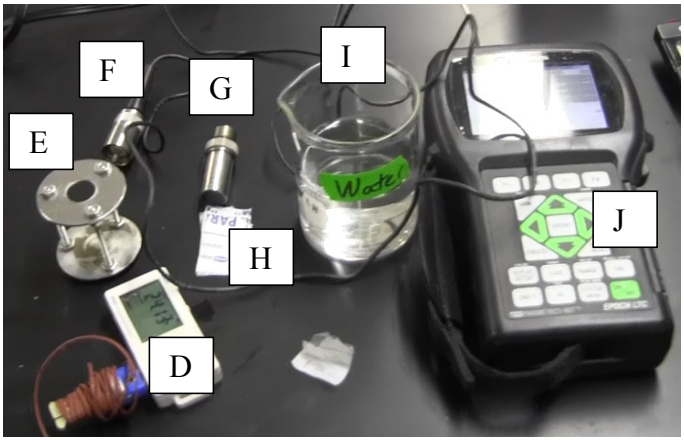

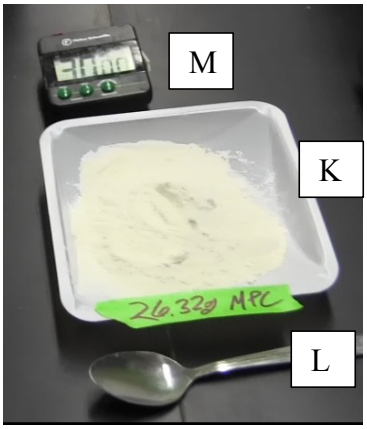

A-Overhead stirrer

B- 1L beaker with 500g deionized water

C-Waterbath

D-Datalogger

E-Transducer holder

F-Connector for transducer to ultrasonic flaw detector

G-1MHz immersion transducer

H-Parafilm

I-Beaker with room temperature

J-Ultrasonic Flaw Detector

K-26.32g powder in container

L-Spoon

M-Timer

Figure A-1 Equipment needed for the ultrasonic flaw detector method

1) Create a new file in the ultrasonic flaw detector (located in the ultrasonic flaw detector manual on pg. 93)

2) Attach data logger to one leg of transducer holder with parafilm

Figure A-2 Datalogger attached to the immersion transducer holder

3) Place transducer in the holder

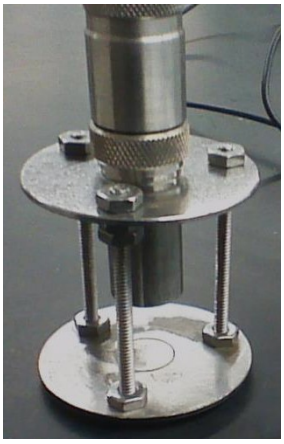

Figure A-3 Immersion transducer in the holder

4) Connect transducer to the ultrasonic flaw detector
5) Place transducer holder in room temperature distilled water (UFD should have a velocity of 1480m/s)
6) Adjust the transducer until two distinct peaks appear (Gain 66 and amplitude greater than or equal to 50)

7) Check that the peaks are in the gate (pg. 61 in the ultrasonic flaw detector manual describes how to position the gate)

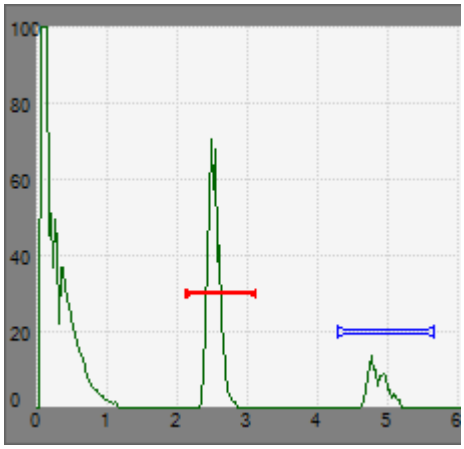

Figure A-4 Ultrasound signal for water

8) Set the ultrasonic flaw detector to record data in mm (located in the ultrasonic flaw detector manual on pg. 31)
9) Push the save button to record the data
10) Set the ultrasonic flaw detector to record data in μs (located in the ultrasonic flaw detector manual on pg. 64)
11) Place the transducer in the beaker of water

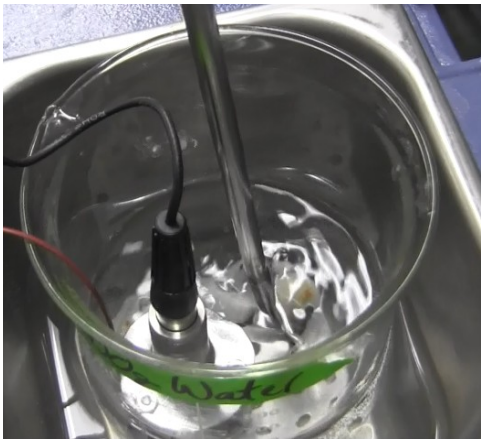

Figure A-5 Immersion transducer and stirrer in the 1L beaker with water

12) Set the overhead stirrer to 400rpm
13) Allows the water to come to the testing temperature ±0.1°C
14) Record the water temperature in a notebook and then push the save button to record the ultrasound data
15) Set the overhead stirrer to 900rpm

16) Add all of the powder within 3 minutes (fold the edges of the powder container together and tap with spoon)

Figure A-6 Addition of powder to the water

17) Separate any clumps that may have collected on the transducer
18) Once there is no more powder on the surface set the overhead stirrer to 400rpm
19) Adjust the gain so that the noise is visible (pg 19-20 in the ultrasonic flaw detector manual describes how to adjust)

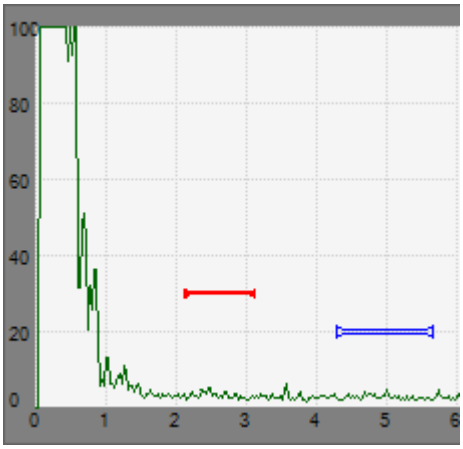

Figure A-7 Ultrasound signal after powder addition

20) Start the timer and push the save button to record the data
21) Push the save button every 15s for 30minutes
22) Clean equipment with distilled water
23) Attach the ultrasonic flaw detector to a computer with a USB cord
24) Open Gageview Pro and copy the data to the correct dataset

25) Export the data to excel
26) Create two new columns between the RDG1 UNITS and RDG2 and label them velocity and relative velocity
27) Calculate distance, velocity, relative velocity, and attenuation

	A	B	C	D	E	F	G	H	I	J	K	L	M
5	**ID**	**TYPE**	**RDG 1**	**RDG 1 UNITS**	**Velocity**	**Relative Velocity**	**RDG 2**	**RDG 2 UNITS**	**RDG 3**	**RDG 3 UNITS**	**RDG 4**	**RDG 4 UNITS**	**Attenuation**
6	001	Distance	18.11	mm	**36.22**		58.0	%	34.56	mm	17.0	%	
7	002	Water	23.993	µs	**1509.61**		63.5	%	45.703	µs	19.75	%	
8	003	0	25.3	µs	1431.62	**0.94834**	4.25	%	43.085	µs	4.0	%	**0.001673789**
9	004	15	24.01	µs	1508.54	0.99929	4.0	%	45.828	µs	3.5	%	0.003686676
10	005	30	18.778	µs	1928.85	1.27772	3.5	%	42.91	µs	3.75	%	-0.00190483
11	006	45	19.015	µs	1904.81	1.26179	4.25	%	40.36	µs	5.0	%	-0.00448699
12	007	60	20.705	µs	1749.34	1.1588	3.75	%	47.165	µs	4.5	%	-0.00503373
13	008	75	28.135	µs	1287.36	0.85278	4.25	%	50.745	µs	4.25	%	0
14	009	90	22.045	µs	1643	1.08836	3.75	%	41.355	µs	4.5	%	-0.00503373
15	010	105	19.352	µs	1871.64	1.23982	3.75	%	46.4	µs	3.75	%	0
16	011	120	24.942	µs	1452.17	0.96195	3.5	%	54.715	µs	4.0	%	-0.00368668
17	012	135	23.095	µs	1568.3	1.03888	3.75	%	43.273	µs	4.75	%	-0.00652647
18	013	150	25.42	µs	1424.86	0.94386	4.0	%	44.87	µs	4.25	%	-0.00167379
19	014	165	24.272	µs	1492.25	0.98851	3.25	%	43.22	µs	3.5	%	-0.00204605
20	015	180	23.508	µs	1540.75	1.02063	3.25	%	49.935	µs	4.5	%	-0.00898461
21	016	195	27.693	µs	1307.91	0.86639	4.0	%	54.308	µs	4.25	%	-0.00167379
22	017	210	19.813	µs	1828.09	1.21097	3.5	%	47.243	µs	4.25	%	-0.00536046
23	018	225	23.422	µs	1546.41	1.02438	3.5	%	39.583	µs	4.25	%	-0.00536046
24	019	240	22.698	µs	1595.74	1.05705	3.75	%	41.99	µs	3.75	%	0
25	020	255	22.717	µs	1594.4	1.05617	4.0	%	54.495	µs	3.75	%	0.001781848
26	021	270	25.345	µs	1429.08	0.94666	3.5	%	48.997	µs	3.75	%	-0.00190483
27	022	285	21.377	µs	1694.34	1.12237	4.75	%	50.215	µs	4.5	%	0.001492745

Figure A-8 Ultrasound data in excel file

Calculations

Distance (E6): =C6*2

*Velocity (E7): =$E$6/C7*1000

*Relative Velocity (F8): =E8/$E$7

*Attenuation (M8): =LN(I8/K8)/$E$6

*Calculations were copied and pasted to the other cells

26) Calculate relative velocity standard deviation and area under the attenuation curve

	A	B	C	D
100	1470	1.00444	0.048839852	0.84219
101	1485	1.00377	0.054894792	0.77801
102	1500	0.99929	0.052409776	0.80478
103	1515	0.99693	0.053724742	0.79601
104	1530	0.99515	0.052264307	0.79492
105	1545	0.98582	0.064655047	0.8769
106	1560	0.99535	0.053572625	0.88671
107	1575	0.99722	0.057592461	0.83374
108	1590	0.99548	0.052924423	0.82888
109	1605	0.99763	0.051577373	0.78376
110	1620	0.99523	0.055461733	0.80279
111	1635	0.9963	0.057246587	0.84531
112	1650	0.99494	0.056534866	0.85336
113	1665	0.99548	0.059669547	0.87153
114	1680	0.99722	0.055365366	0.86276
115	1695	0.99597	0.056236387	0.83701
116	1710	0.99461	0.049047267	0.78963
117	1725	1.00167	0.059621321	0.81501
118	1740	0.99473	0.05695756	0.87434
119	1755	0.99502	0.053597217	0.82916
120	1770	0.99589	0.058093157	0.83768
121	1785	0.99502	0.052231997	0.82744
122	1800	1.013	0.051208516	**0.7758**
123		**0.00583**		**61.6343**

Figure A-9 Ultrasound data with the relative velocity standard deviation from 900-1800s and area under the attenuation curve calculated

Calculations

Relative velocity standard deviation (900-1800s) (B123): =STDEV.S(B62:B122)

Area under the attenuation curve (D123): =SUM(D3:D122)

D122: =AVERAGE(D121:122)*15 (the same calculation was used starting with D2 and D3)

28) Identify peak height and peak time (select attenuation and time, sort by largest to smallest for attenuation)

	A	B
1	**Attenuation**	**Time**
2	**0.067218244**	**1215**
3	0.066203624	1200
4	0.064655047	1545
5	0.063895117	1065
6	0.063725159	1275
7	0.063451899	1455
8	0.063263716	1110
9	0.062873199	1290
10	0.062499869	1350
11	0.062337084	945
12	0.061419756	1170
13	0.061002062	1035
14	0.06080899	1005
15	0.060072705	1080
16	0.059885525	1050
17	0.059885525	1095
18	0.059745967	1125
19	0.059669547	1665
20	0.059621321	1725
21	0.058469365	1260
22	0.058093157	1770
23	0.057853172	1410
24	0.057592461	1575

Figure A-10 Ultrasound data with the peak height (A2) and peak time (B2)

Appendix B - SAS code for chapter 5

Relative velocity standard deviation (SD)
Area under the attenuation curve (Area)
Peak height (PH)
Peak time (PT)

```
/*One way CRD and 2-way factorial   */
 /*1. Only for 40C   */
data onet;
input Lot$ Type$ SD Area PH PT;
datalines;
15054 A     0.011323412 66.02038707 0.073666113 1350
15054 A     0.008766014 70.46409005 0.07268374  885
15047 A     0.002582113 64.10333105 0.060910965 465
15047 A     0.000796985 63.07593695 0.062983285 495
15044 A     0.009132587 68.74187525 0.070114425 870
15044 A     0.010279105 63.5917981  0.067635797 900
15056 B     0.011323412 66.02038707 0.073666113 1350
15056 B     0.008766014 70.46409005 0.07268374  885
15048 B     0.016624259 65.43624644 0.071368118 1095
15048 B     0.020038277 56.79802236 0.068769621 1080
15049 B     0.000957032 71.19776836 0.067003717 495
15049 B     0.001040817 71.84479497 0.065427268 615
14357 C     0.03081318  40.70616536 0.064564402 1515
14357 C     0.033271827 38.7627225  0.066356919 1740
15056 C     0.067444868 17.6658489  0.056207277 1800
15056 C     0.078226084 13.94241811 0.035447919 1755
15048 C     0.041235882 30.0620271  0.065517148 1785
15048 C     0.046186741 29.97212122 0.062424557 1800
15044 C     0.103905878 4.981050929 0.027969306 1155
15044 C     0.099111834 6.408472976 0.024000009 1725
15020 D     0.024975024 28.83075315 0.059096552 1785
15020 D     0.079656968 13.14418976 0.038609289 1770
;
run;

proc print data=onet;
run;

proc glimmix data=onet;
* GLIMMIX for everything else;
      class Type;
      model SD = Type/solution;
      lsmeans Type/ pdiff adjust=tukey cl plot=meanplot(ascending cl);
      output out=residuals residual=residual predicted=predicted;
run;

proc glimmix data=onet;
* GLIMMIX for everything else;
      class Type;
      model Area=Type/solution;
      lsmeans Type/cl pdiff adjust=tukey plot=meanplot(ascending cl);
      output out=residuals residual=residual predicted=predicted;
run;
```

```
proc glimmix data=onet;
* GLIMMIX for everything else;
      class Type;
      model PH = Type/solution;
      lsmeans Type/ pdiff adjust=tukey cl plot=meanplot(ascending cl);
      output out=residuals residual=residual predicted=predicted;
run;
proc glimmix data=onet;
* GLIMMIX for everything else;
      class Type;
      model PT = Type/solution;
      lsmeans Type/ pdiff adjust=tukey cl plot=meanplot(ascending cl);
      output out=residuals residual=residual predicted=predicted;
run;

/*2. Compare both 40C and 48C   */
data twot;
input Lot$ Type$ Temp$ SD Area PH PT ;*Composition*;
datalines;
15054 A     40    0.011323412 66.02038707 0.073666113 1350
15054 A     40    0.008766014 70.46409005 0.07268374  885
15047 A     40    0.002582113 64.10333105 0.060910965 465
15047 A     40    0.000796985 63.07593695 0.062983285 495
15044 A     40    0.009132587 68.74187525 0.070114425 870
15044 A     40    0.010279105 63.5917981  0.067635797 900
15056 B     40    0.011323412 66.02038707 0.073666113 1350
15056 B     40    0.008766014 70.46409005 0.07268374  885
15048 B     40    0.016624259 65.43624644 0.071368118 1095
15048 B     40    0.020038277 56.79802236 0.068769621 1080
15049 B     40    0.000957032 71.19776836 0.067003717 495
15049 B     40    0.001040817 71.84479497 0.065427268 615
14357 C     40    0.03081318  40.70616536 0.064564402 1515
14357 C     40    0.033271827 38.7627225  0.066356919 1740
15056 C     40    0.067444868 17.6658489  0.056207277 1800
15056 C     40    0.078226084 13.94241811 0.035447919 1755
15048 C     40    0.041235882 30.0620271  0.065517148 1785
15048 C     40    0.046186741 29.97212122 0.062424557 1800
15044 C     40    0.103905878 4.981050929 0.027969306 1155
15044 C     40    0.099111834 6.408472976 0.024000009 1725
15020 D     40    0.024975024 28.83075315 0.059096552 1785
15020 D     40    0.079656968 13.14418976 0.038609289 1770
15054 A     48    0.007377658 86.16556117 0.069267723 1260
15054 A     48    0.009163627 84.12907931 0.070402093 705
15047 A     48    0.004895083 85.1983153  0.066002499 780
15047 A     48    0.0058787   78.90745186 0.070550174 525
15044 A     48    0.009376973 80.95159304 0.066892743 1035
15044 A     48    0.008531233 88.15729453 0.07849875  1605
15056 B     48    0.00605565  90.85558485 0.077471226 1800
15056 B     48    0.008999933 71.21090095 0.073962881 1680
15048 B     48    0.009909504 80.77021769 0.076317772 840
15048 B     48    0.003615195 77.42278959 0.07798769  1440
15049 B     48    0.009070433 102.7775014 0.081444984 1335
15049 B     48    0.003139114 104.8400814 0.080030888 1065
14357 C     48    0.013045074 57.64042857 0.068574923 1110
14357 C     48    0.013194109 62.72951982 0.063559225 930
15056 C     48    0.019099333 60.03010553 0.073880933 1515
15056 C     48    0.033287593 36.21966476 0.071365931 1800
```

```
15048 C     48    0.02212359  39.63745374 0.065286176 1635
15048 C     48    0.008818492 57.90332744 0.065844395 1395
15044 C     48    0.064972397 30.76904315 0.067025921 1755
15044 C     48    0.010234995 66.83693977 0.068186247 1095
15020 D     48    0.019176889 49.13118327 0.066756011 1320
15020 D     48    0.016588745 54.12506389 0.070898112 1260
;
run;

proc print data=twot;
run;

proc glimmix data=twot;
* GLIMMIX for everything else;
      class Type Temp;
      model SD = Type Temp Type*Temp/solution;
      lsmeans Type Temp Type*Temp/cl plot=meanplot(ascending cl);
      output out=residuals residual=residual predicted=predicted;
run;

proc glimmix data=twot;
* GLIMMIX for everything else;
      class Type Temp;
      model Area=Type Temp Type*Temp/solution;
      lsmeans Type Temp Type*Temp/cl plot=meanplot(ascending cl);
      output out=residuals residual=residual predicted=predicted;
run;
proc glimmix data=twot;
* GLIMMIX for everything else;
      class Type Temp;
      model PH = Type Temp Type*Temp/solution;
      lsmeans Type Temp Type*Temp/cl plot=meanplot(ascending cl);
      output out=residuals residual=residual predicted=predicted;
run;
proc glimmix data=twot;
* GLIMMIX for everything else;
      class Type Temp;
      model PT = Type Temp Type*Temp/solution;
      lsmeans Type Temp Type*Temp/cl plot=meanplot(ascending cl);
      output out=residuals residual=residual predicted=predicted;
run;

/*1. Only for 48C   */
data onet;
input Lot$ Type$ SD Area PH PT;
datalines;
15054 A     0.007377658 86.16556117 0.069267723 1260
15054 A     0.009163627 84.12907931 0.070402093 705
15047 A     0.004895083 85.1983153  0.066002499 780
15047 A     0.0058787   78.90745186 0.070550174 525
15044 A     0.009376973 80.95159304 0.066892743 1035
15044 A     0.008531233 88.15729453 0.07849875  1605
15056 B     0.00605565  90.85558485 0.077471226 1800
15056 B     0.008999933 71.21090095 0.073962881 1680
15048 B     0.009909504 80.77021769 0.076317772 840
15048 B     0.003615195 77.42278959 0.07798769  1440
15049 B     0.009070433 102.7775014 0.081444984 1335
```

```
15049 B     0.003139114 104.8400814 0.080030888 1065
14357 C     0.013045074 57.64042857 0.068574923 1110
14357 C     0.013194109 62.72951982 0.063559225 930
15056 C     0.019099333 60.03010553 0.073880933 1515
15056 C     0.033287593 36.21966476 0.071365931 1800
15048 C     0.02212359  39.63745374 0.065286176 1635
15048 C     0.008818492 57.90332744 0.065844395 1395
15044 C     0.064972397 30.76904315 0.067025921 1755
15044 C     0.010234995 66.83693977 0.068186247 1095
15020 D     0.019176889 49.13118327 0.066756011 1320
15020 D     0.016588745 54.12506389 0.070898112 1260
;
run;

proc print data=onet;
run;

proc glimmix data=onet;
* GLIMMIX for everything else;
      class Type;
      model SD = Type/solution;
      lsmeans Type/ pdiff adjust=tukey cl plot=meanplot(ascending cl);
      output out=residuals residual=residual predicted=predicted;
run;

proc glimmix data=onet;
* GLIMMIX for everything else;
      class Type;
      model Area=Type/solution;
      lsmeans Type/cl pdiff adjust=tukey plot=meanplot(ascending cl);
      output out=residuals residual=residual predicted=predicted;
run;
proc glimmix data=onet;
* GLIMMIX for everything else;
      class Type;
      model PH = Type/solution;
      lsmeans Type/ pdiff adjust=tukey cl plot=meanplot(ascending cl);
      output out=residuals residual=residual predicted=predicted;
run;
proc glimmix data=onet;
* GLIMMIX for everything else;
      class Type;
      model PT = Type/solution;
      lsmeans Type/ pdiff adjust=tukey cl plot=meanplot(ascending cl);
      output out=residuals residual=residual predicted=predicted;
run;
```